# Turbulent Flow Separation in 3-D Asymmetric Diffusers

Elbert Jeyapaul

NASA postdoctoral fellow,
Langley research center.

11/29/2011

# Outline

# Acknowledgements

1. Prof. Paul Durbin at Iowa state university
2. Chris Rumsey at NASA LaRC
3. Colleagues, Jongwook Joo, Alberto Passalaqua, Sunil Arolla.
4. Funding from NASA cooperative agreement NNX07AB29A and postdoctoral program.

# Outline

# Outline

# Outline

# Outline

# Outline

# Outline

# Outline

# Objective

1. Understand the fluid dynamics of 3–D turbulent separation in diffusers
2. Predicting complex 3–D turbulent separated flows with a reasonable cost
   - Identify parameters that sensitize eddy-viscosity models to flow separation
   - Develop an improved RANS model

# Motivation

- All linear eddy-viscosity models (LEVM) are qualitatively incorrect in predicting separation in 3-D asymmetric diffusers.
- Flow separation in internal flows occur in a number of engineering devices, gas turbine transition ducts, compressor, LP turbine, etc. Currently such flows can only be predicted by eddy-resolving simulations, which are expensive.

# Scope & Characteristics

- 3-D asymmetric diffusers is used to study internal flow separation that is induced by Adverse pressure gradients. The flow is limited to;
  - Statistically-steady separation
  - Incompressible flow
  - Inlet Reynolds number of 10,000 & 20,000.
- Separation, the breakdown of boundary layer is defined as surface of zero streamwise velocity.
- Separation occurs along characteristic curves that connect singular points. Not at $\tau_{wall} = 0$ as in 2-D.

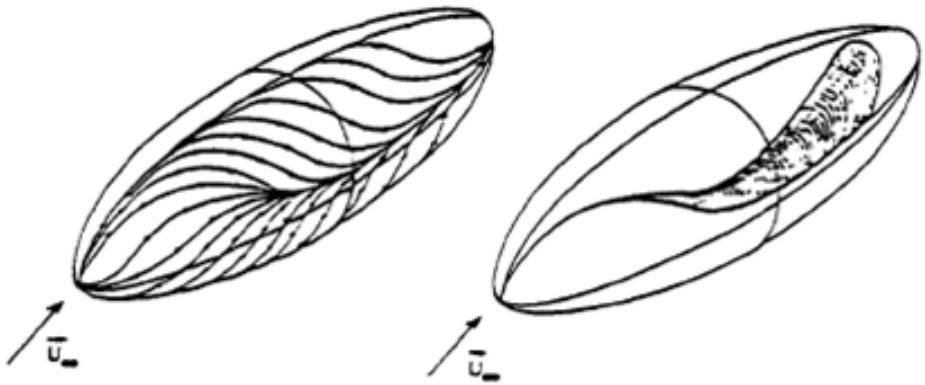

*Convergence of skin friction lines is a necessary criteria for separation – Lighthill (1963)*

# Baseline Geometry

- An asymmetrically-sloped 3–D diffuser of Cherry et al(2008) has been used as a test configuration for this study (Diffuser 1).
- A fully-developed turbulent flow enters the diffuser at a Reynolds number of 10,000 based on inlet channel height and bulk velocity.
- Area expansion ratio is 4.8

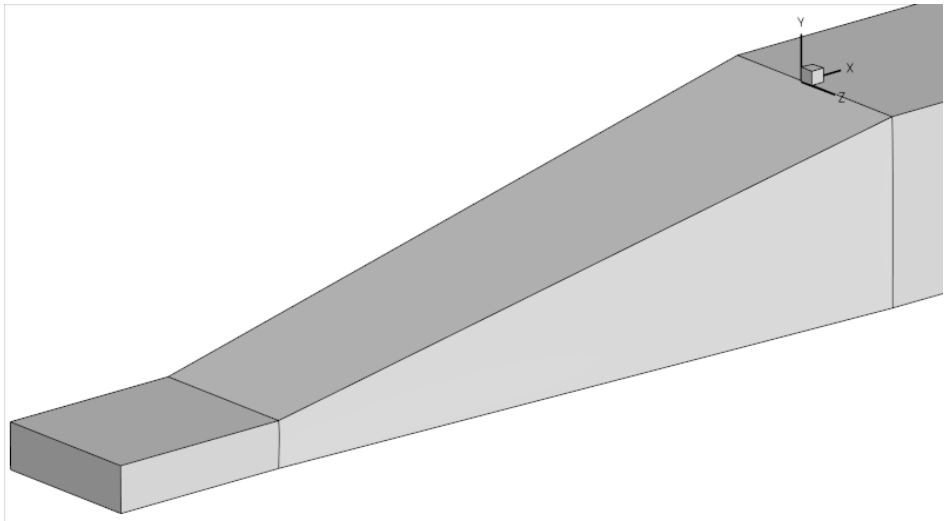

Top

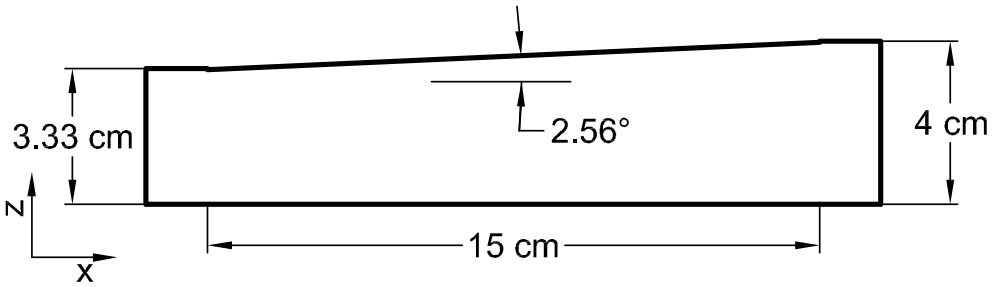


Side

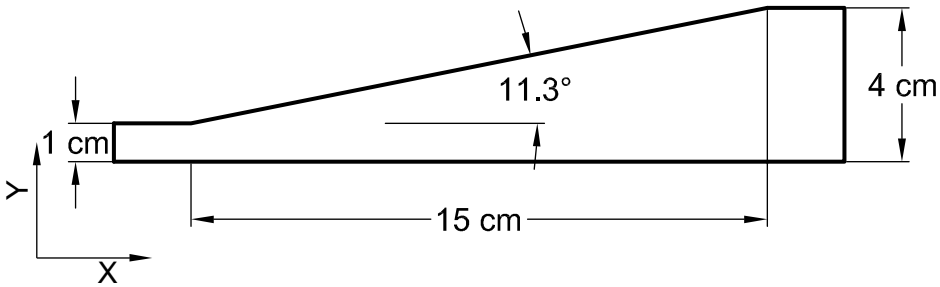

# Grid dependence

- Flow domain consists of inlet channel to diffuser and an outlet transition section.
- Hexahedral cells are used to discretize the domain. For the DES, two grids were generated.
  **COARSE** $357 \times 41 \times 61$, Near-wall expansion=1.1, $\Delta y_+ = 7$, $\Delta x_+ = 1640$ and $\Delta z_+ = 160$
  **FINE** $296 \times 61 \times 101$, Near-wall expansion=1.01, $\Delta y_+ = 0.6$, $\Delta x_+ = 12$ and $\Delta z_+ = 36$
- Separation bubble predicted by DES using FINE grid was closer to experiments, hence chosen.

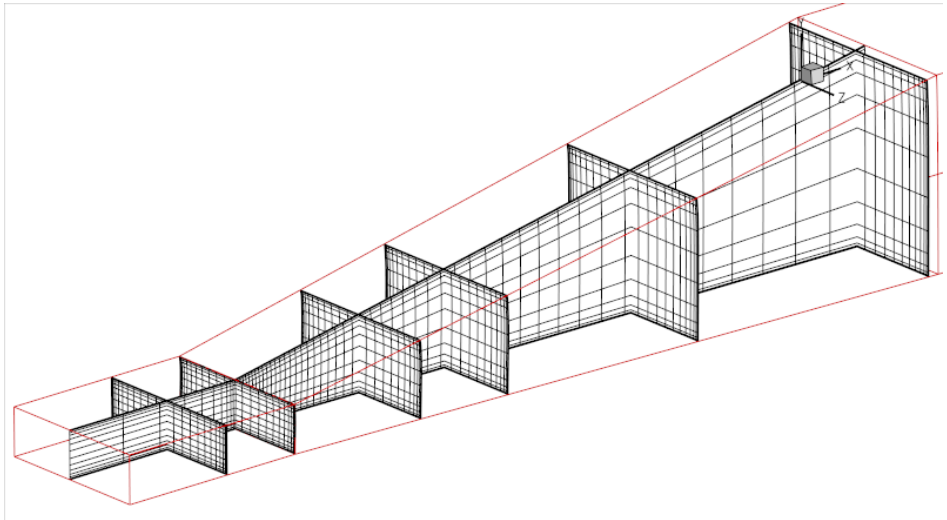

RANS

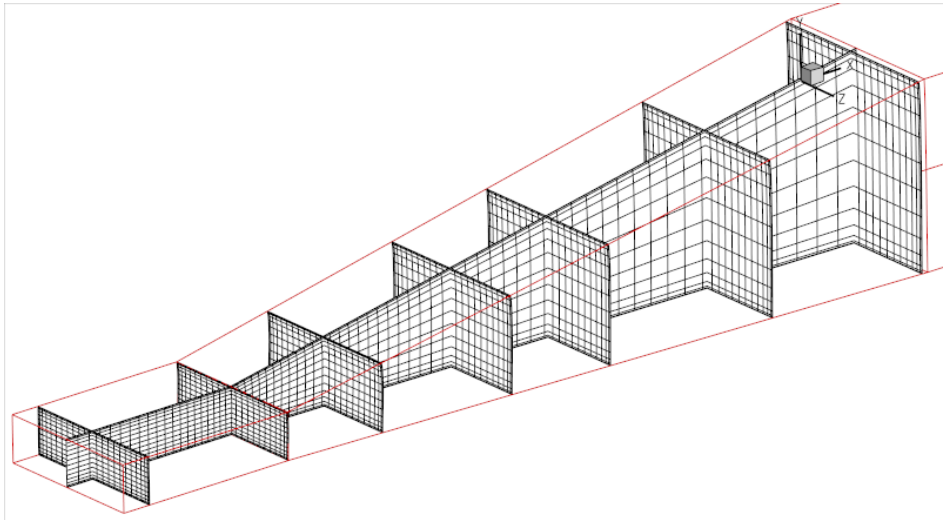

DES

# Solver Numerics

**SUMB**: DES were conducted using this parallelized Finite volume based compressible Navier-Stokes solver.

- Structured Multiblock
- Central + matrix dissipation for flux computations
- 5-stage RK smoother for flow and ADI smoother for turbulence quantities
- 3W-cycle multigrid

**OpenFOAM**: LES and RANS were simulated using this parallelized unstructured finite volume code. The incompressible solver is used with the following salient features.

- Conjugate gradient linear solver for pressure
- Bi-conjugate gradient solver for momentum
- PISO algorithm with two corrector steps
- To improve convergence, a limited central differencing is used for convective terms
- Central difference for gradient and Laplacian terms
- Second-order backward scheme for time derivatives.
- For RANS, the SIMPLE method is used with Gauss-Seidel smoother.

# Inlet profile generation

DES

- Precursor LES was conducted to generate time varying data for a fully-developed turbulent flow for the following scalars $\overline{U}, \overline{V}, \overline{W}, k_{sgs}, \omega_{sgs}$
- The sub-grid scale turbulence quantities are computed as

$$k_{sgs} = \sqrt{\frac{2}{C_\mu}} \nu_{sgs} |S| \quad ; \quad \omega_{sgs} = \frac{\epsilon}{k} = \sqrt{2C_\mu} S$$

- Averaged flow field indicate secondary flow patterns with a pair of counter rotating vortices at each corner.

LES

- Recirculating inlet boundary condition was used to generate fully–developed turbulent inflow. No precursor simulation was necessary.

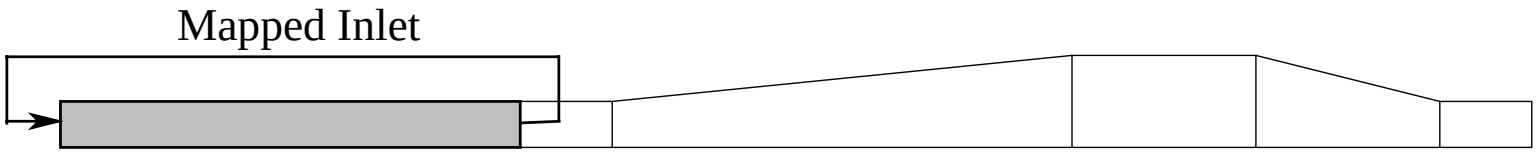


*Inlet mapping is over 10H, H is the channel height*

# DES flow resolution

- More than 50% of the turbulent energy is resolved
- Turbulent viscosity is within the acceptable range.
- The flow is “statistically stationary”, as no coherent structures are found, and URANS results are same as steady-RANS
  $\Rightarrow$ Reynolds averaging is synonymous with time averaging.

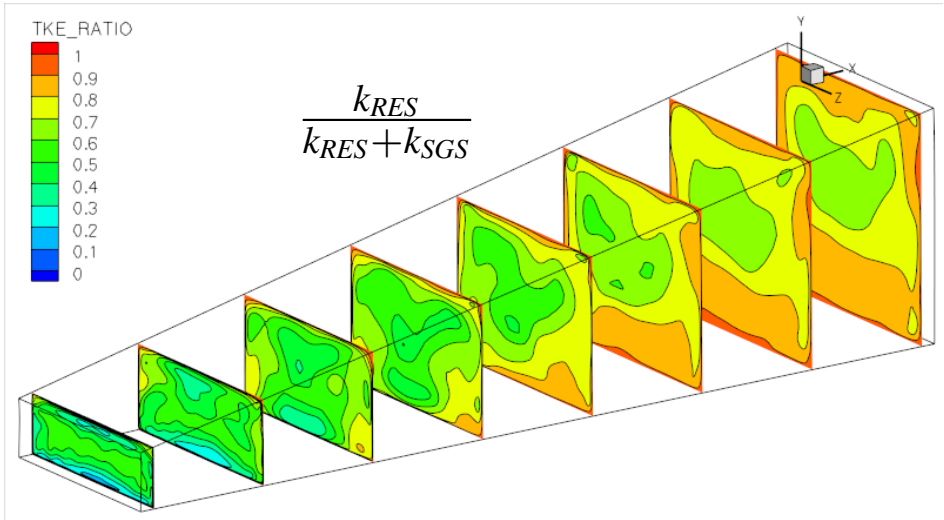


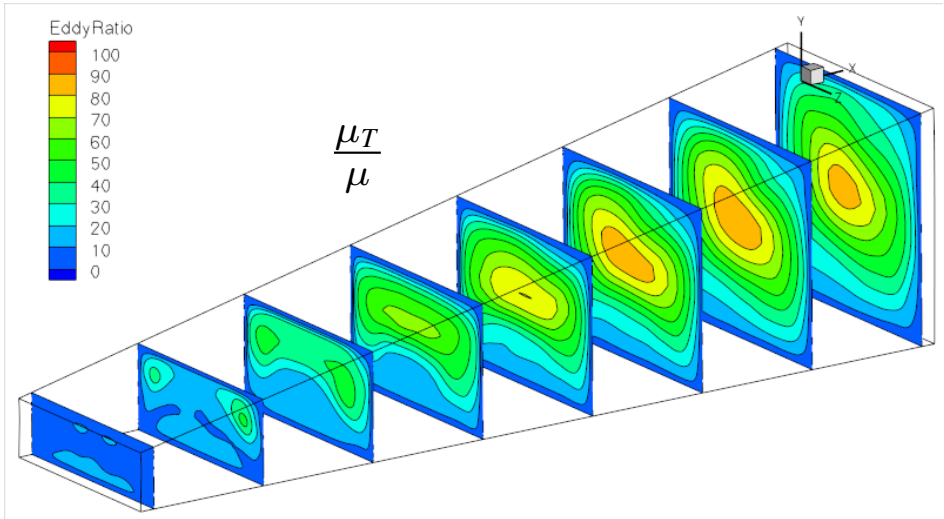

# DES validation – Mean flow

- Baseline diffuser has been used to validate the DES.
- The time averaged DES results predict accurately the mean flow streamwise velocity.
- The secondary flow could not be validated, due to the low accuracy of the MRI experimental data.

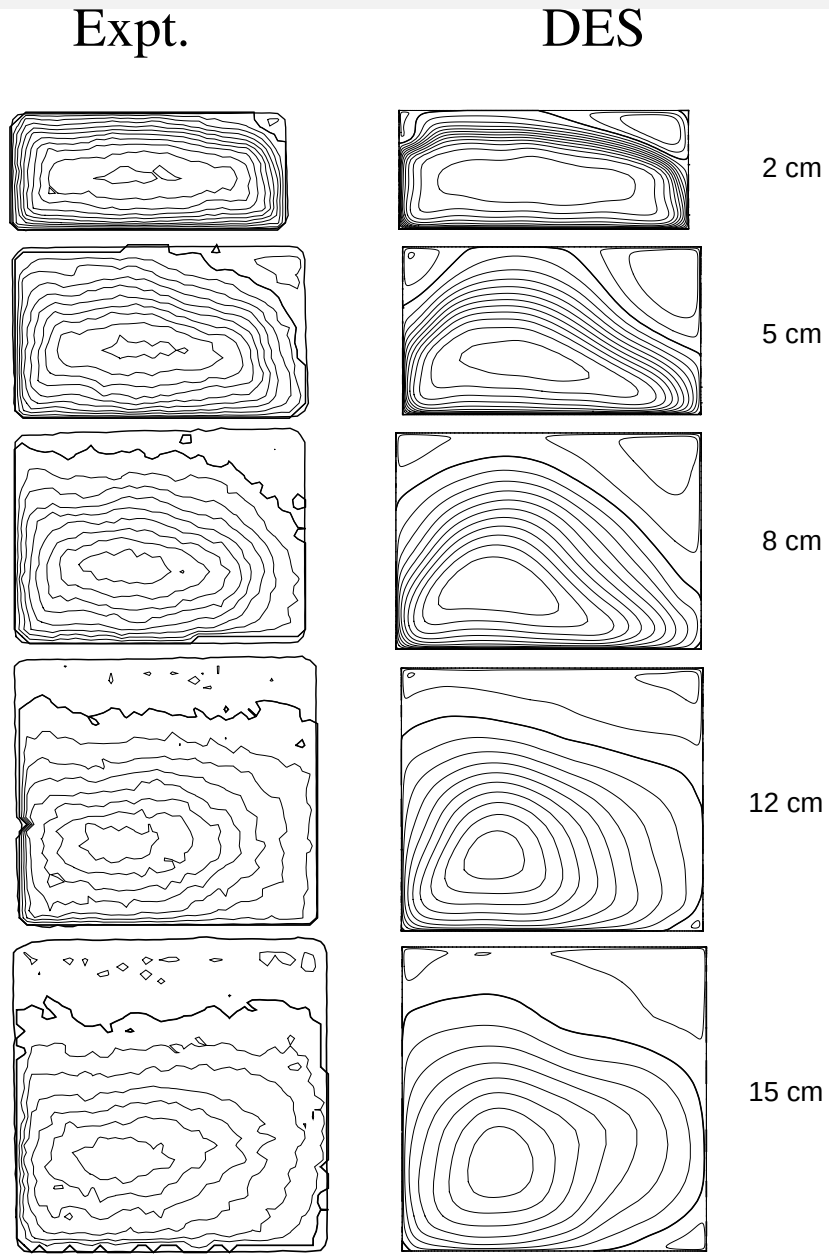

# Secondary flow

- Secondary flow pattern predicted by DES and SST models are comparable close to the inlet, but they develop quite differently downstream.
- Vortices originate from singularities (saddle node) on the sloped walls and interact downstream.
- As the flow relaxes from the large initial deceleration down the duct, the RANS ($k-\varepsilon$, $k-\omega$, SST and $v^2-f$) models fail in the recovery region.

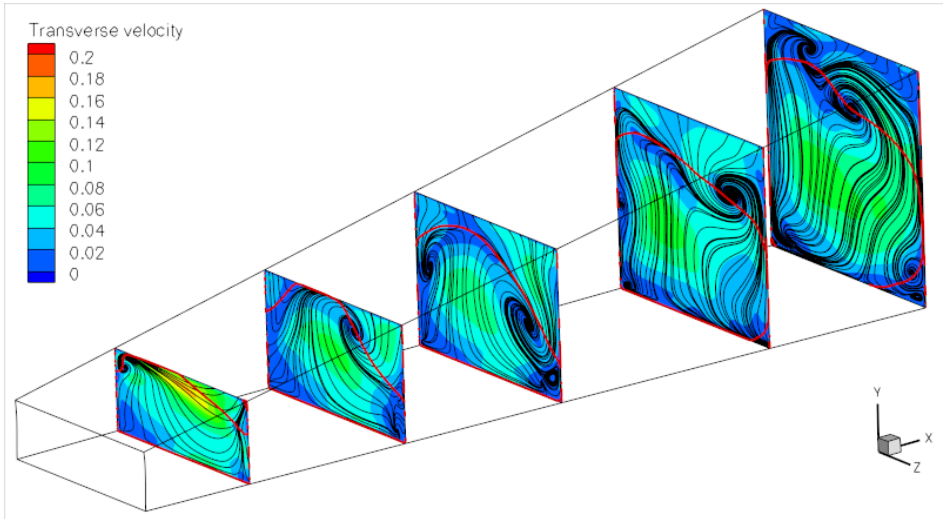


DES

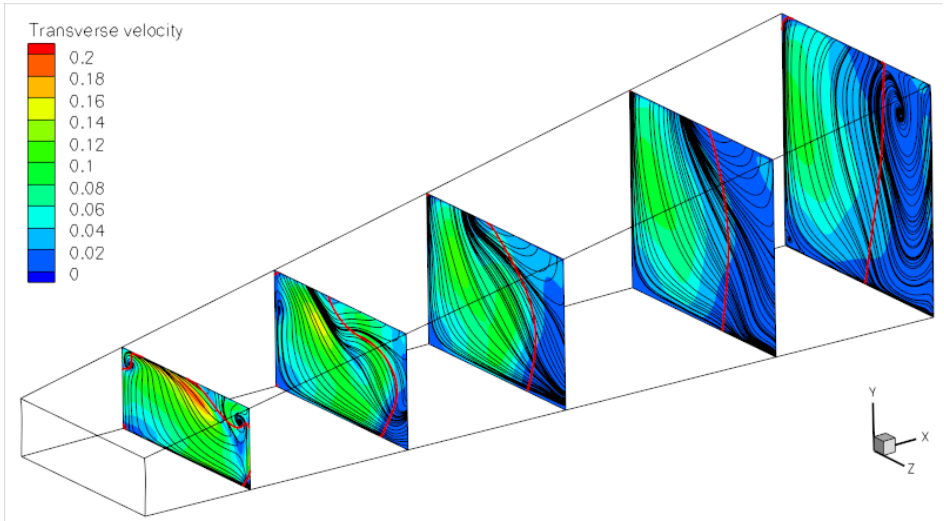


$k-\omega$ SST

# Outline

# Geometry Generation

- A Quasi one-dimensional analysis was used to generate the family.
- The has the same area expansion ratio as that of Obi et al(1993) 2-D diffuser.
- A more accurate comparison can be made when the $dp/dx$ is the same as that of Obis at every x location. A reference diffuser was chosen and used to generate the family of diffusers parameterized by inlet $\mathcal{R}$.

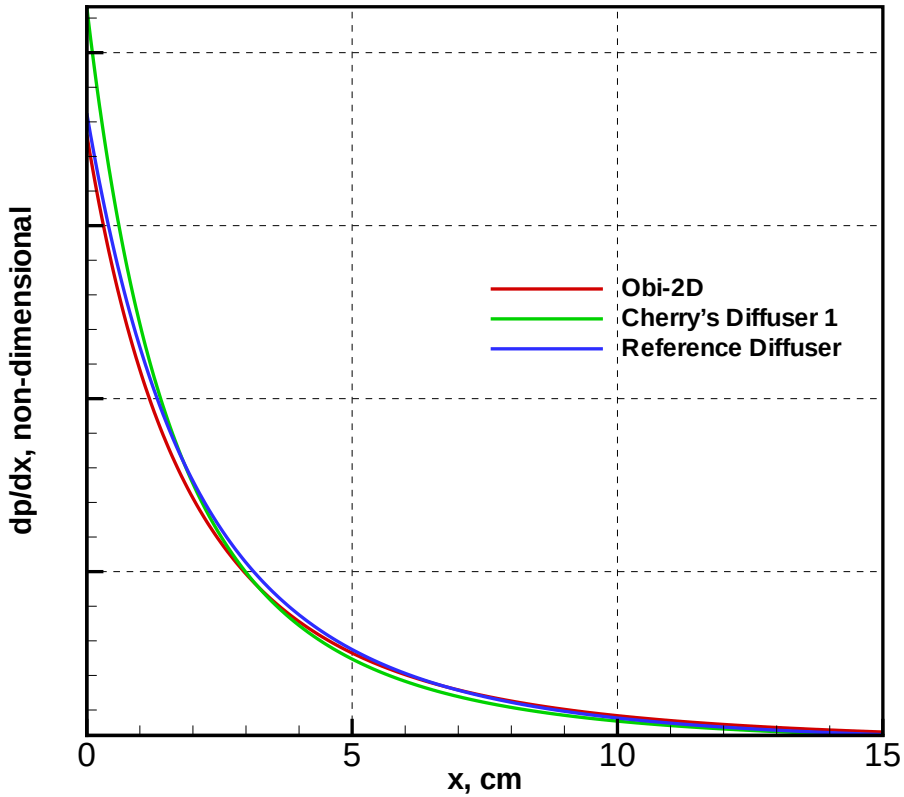


Bernoulli's equation:

$$\frac{dp}{dx} = \frac{\rho Q^2}{A^3}\frac{dA}{dx}; \qquad \frac{dp_1}{dx} = \frac{dp_2}{dx} \implies A_1 = A_2, \forall x$$

# Geometry of series

- With a reference diffuser the family has been generated. $y_r = z_r = 1.34, \alpha_r = tan(11.3°), \beta_r = tan(2.56°)$
- The fluid viscosity has been modified to have the same Reynolds number.
- The cross-sectional area is;

$$A = (y_0 + \alpha x)(z_0 + \beta x)$$
$$= (y_r + \alpha_r x)(z_r + \beta_r x)$$

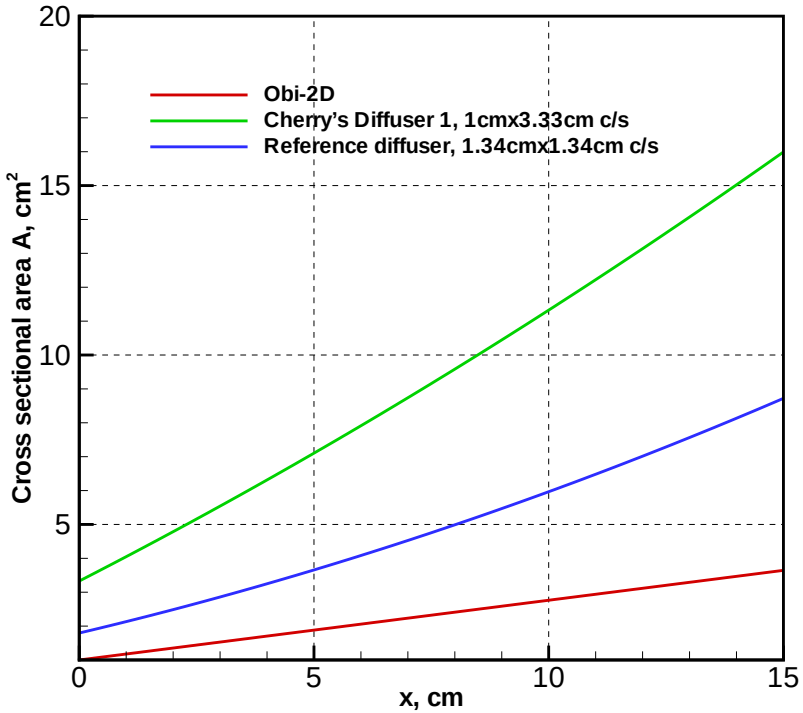


A solution to this equation gives a series dependent on diffuser inlet $\mathcal{R}$,

$$y_0 = y_r\sqrt{\frac{\mathcal{R}_r}{\mathcal{R}}},\ z_0 = z_r\sqrt{\frac{\mathcal{R}}{\mathcal{R}_r}},$$
$$\alpha = \alpha_r\sqrt{\frac{\mathcal{R}_r}{\mathcal{R}}},\ \beta = \beta_r\sqrt{\frac{\mathcal{R}}{\mathcal{R}_r}}$$

# Geometry set

- The series of diffusers have a pressure gradient similar to Obi's 2-D diffuser.
- The effect of secondary pressure gradient on flow prediction can be studied, which varies across $\mathcal{R}$'s.
- All the below cases were simulated using RANS models and eddy-resolving simulations

| **Aspect Ratio** | **1** | **1.5** | **2** | **2.5** | **3** |
|---|---|---|---|---|---|
| Side angle $\theta_s$,deg | 2.56 | 3.13 | 3.6 | 4.04 | 4.43 |
| Top angle $\theta_t$,deg | 11.3 | 9.27 | 8.04 | 7.2 | 6.58 |
| Inlet c/s, w×h cm | 1.34×1.34 | 1.64×1.09 | 1.89×0.95 | 2.12×0.85 | 2.32×0.77 |
| Hydraulic dia. $\phi$ | 1.34 | 1.31 | 1.26 | 1.21 | 1.16 |
| Exit c/s, w×h cm | 2.01×4.38 | 2.46×3.56 | 2.84×3.08 | 3.18×2.75 | 3.48×2.51 |
| Kin. Visc. $\nu$, $m^2/s$ | 1.34e-5 | 1.31e-5 | 1.26e-5 | 1.21e-5 | 1.16e-5 |

Table: Comparison of parameters of family of diffusers sharing same area distribution or dp/dx

# RANS simulations

- RANS models (including $k-\varepsilon$ and $v^2-f$) predict separation to move from top to side at about AR2. Indicating the models to be sensitive to transverse pressure gradients.
- As the adverse pressure gradient is the same for all cases, the separation surface remains on side wall, as verified by DES. A 'transition' in separation surface is not observed in DES.

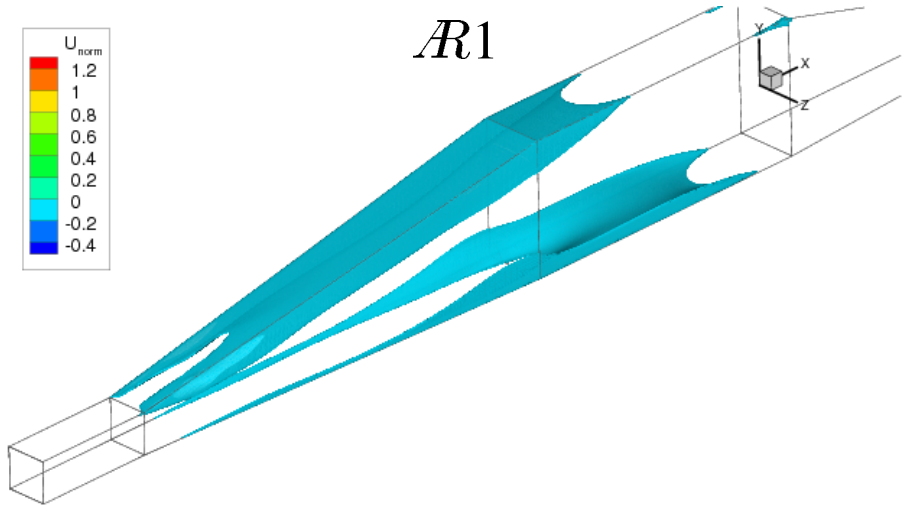


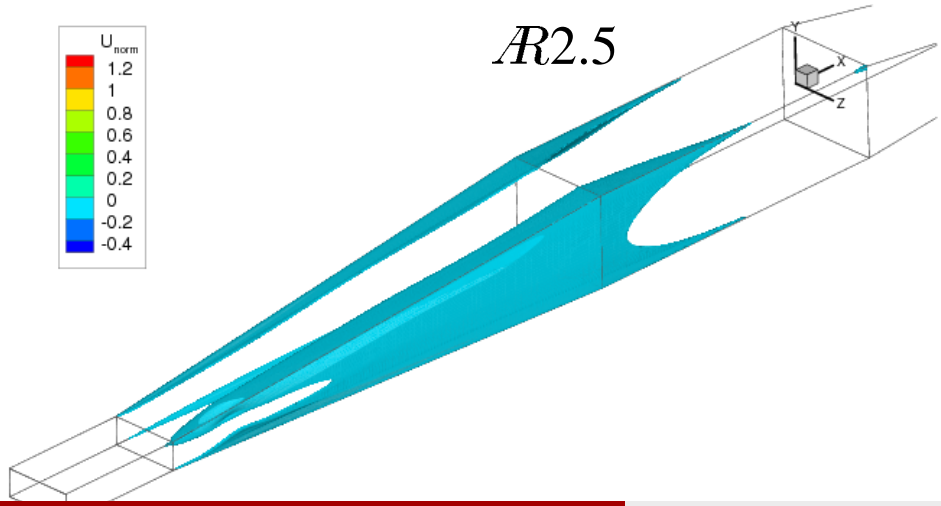


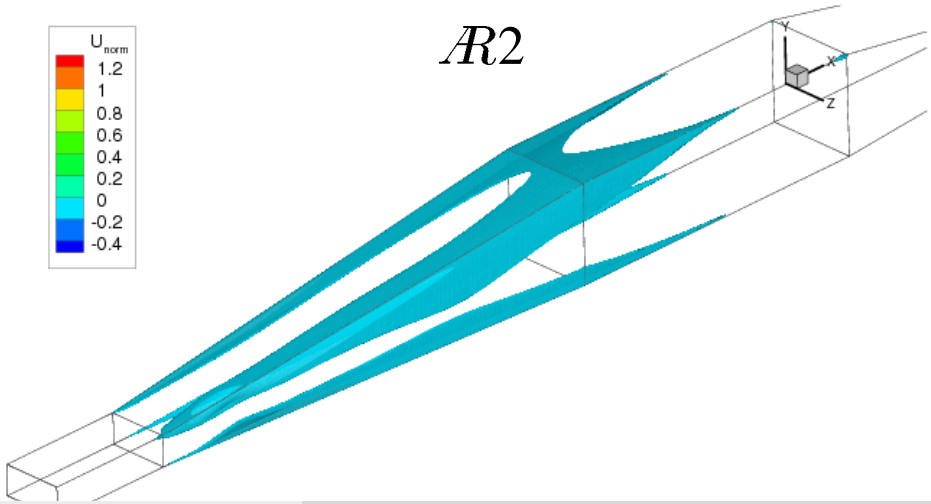

# DES predictions

- The flow separates on the side slope for both cases. The $\mathcal{R}2.5$ indicate higher unsteadiness.
- The $\mathcal{R}2.5$ case has been further investigated for secondary flow features as predicted by DES and SST models.

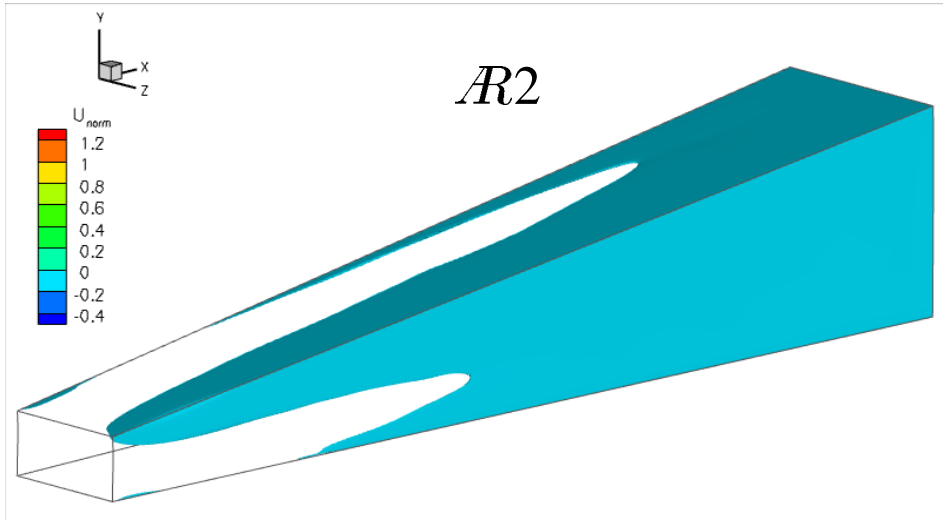


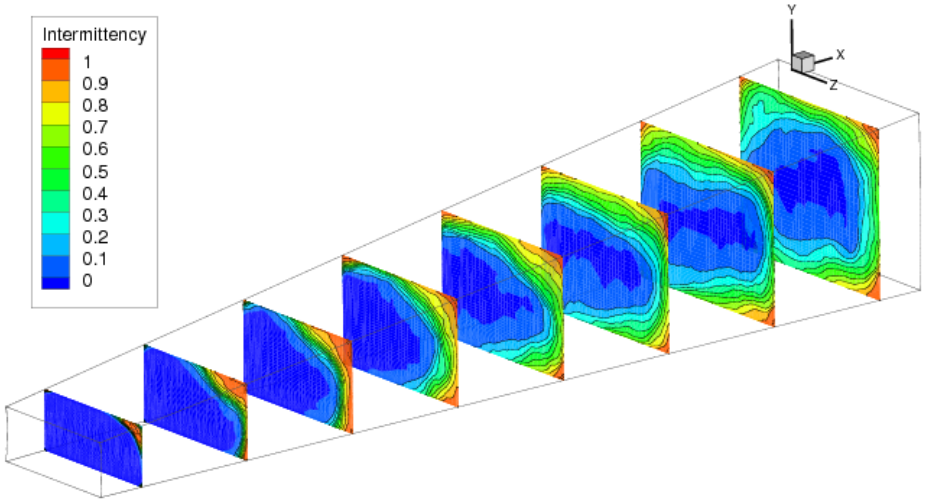


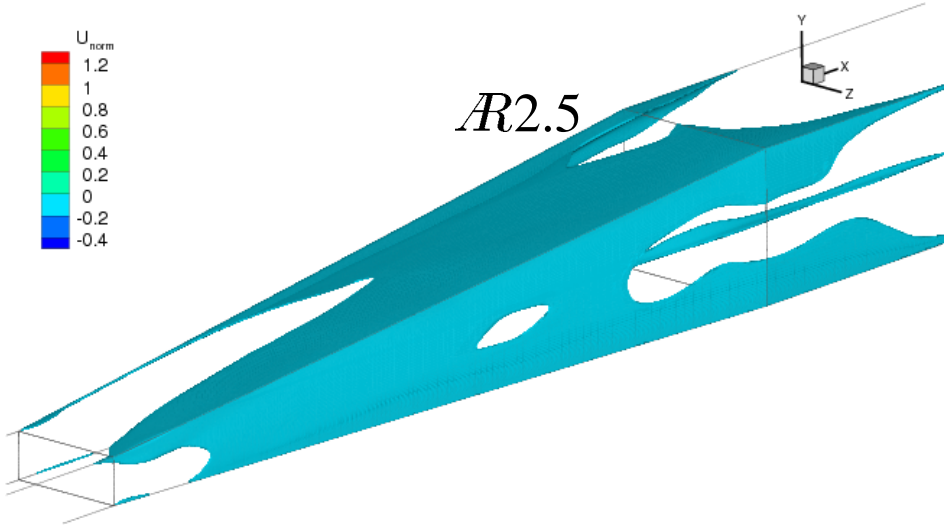


*Intermittency shows % of flow moving downstream to upstream*

# Animation of separation surface of $\mathcal{R}2.5$

Figure: Streamwise velocity variation over one flow-through time.

# Wall stress lines in $\mathcal{R}2.5$

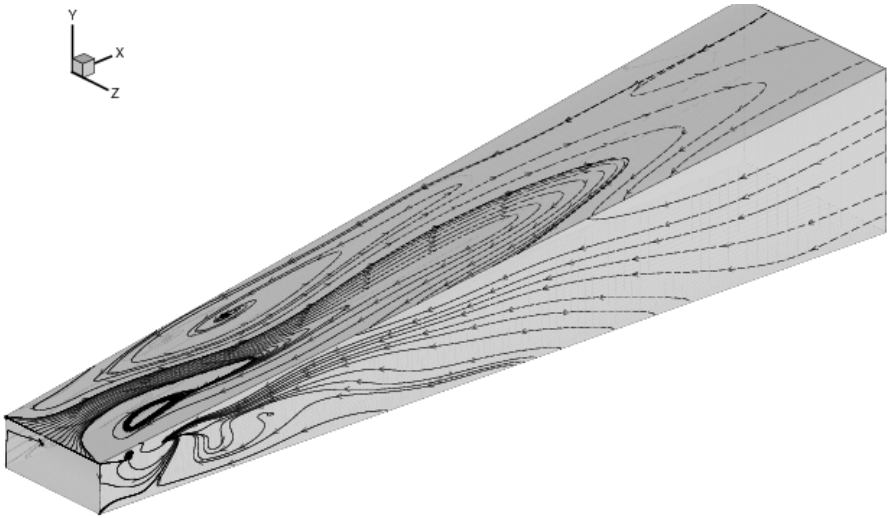


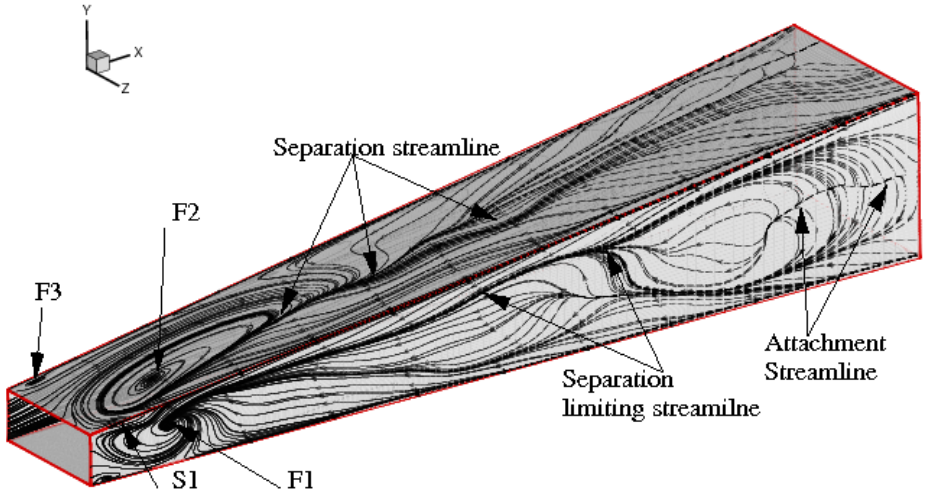


*SST* *DES*

- The singularities close to the inlet are accurately captured by SST model.
- The streamlines predicted downstream by SST lack in detail. The flow singularities occur at geometric singularities.
- Singular points(3 foci and 1 saddle node) move close to the inlet as $\mathcal{R}$increases.

# 3–D flow structures in $\mathcal{R}2.5$

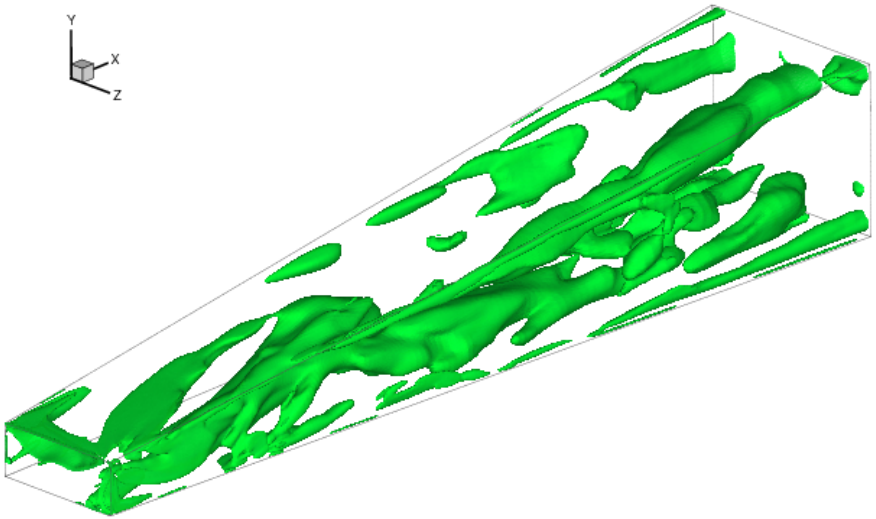


*Isosurfaces of the invariant of velocity, $Q(|\mathbf{\Omega^2}| - |\mathbf{S^2}|)$ show a strong vortex on the top-right edge.*

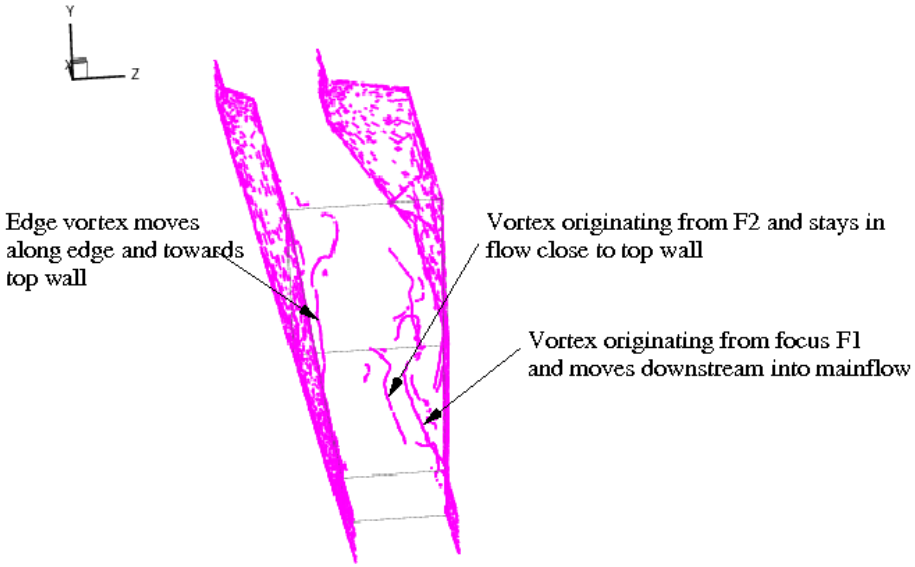


*Major vortex cores in diffuser*

- Vortices originate from the foci on the sloped walls. The Q contours indicate the vortices originating from F1 and F2 to dominate the flow.
- The vortices from both walls interact downstream.

# Secondary flow in $\mathcal{R}2.5$

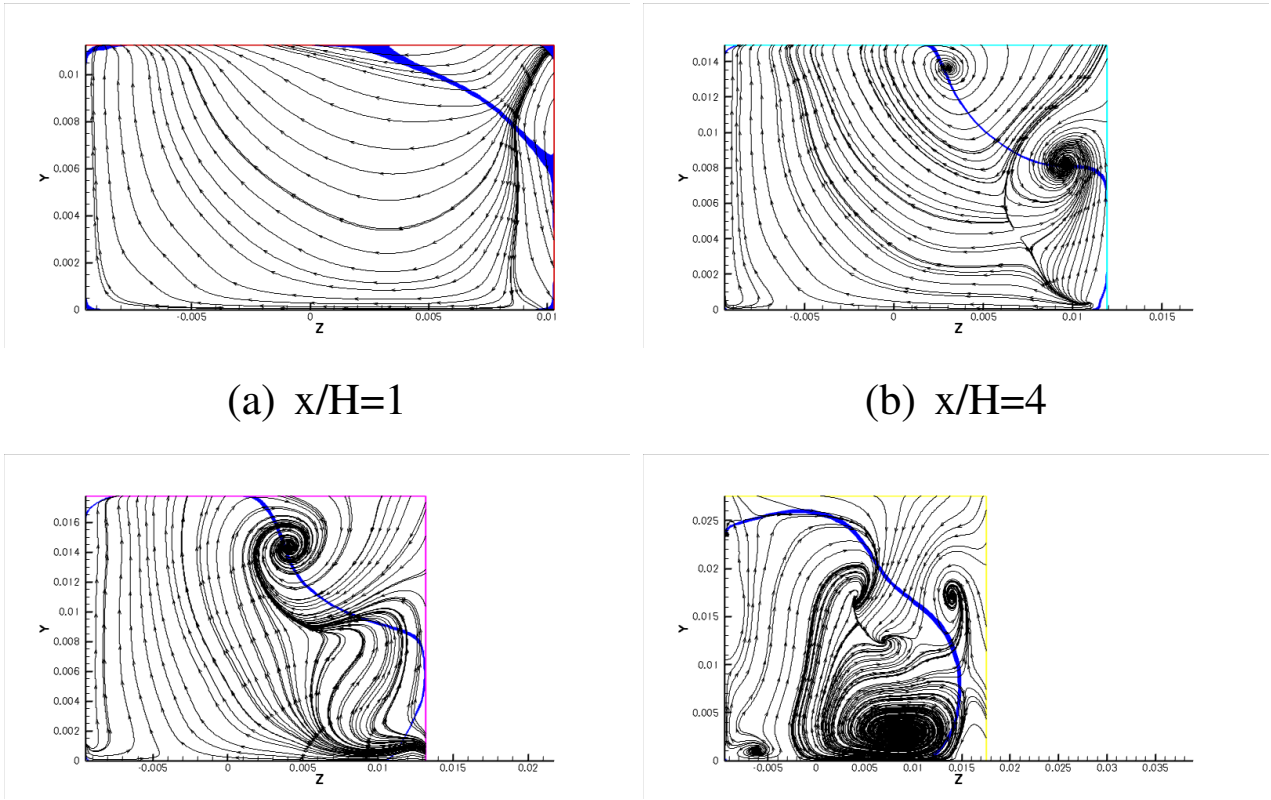


(a) x/H=1 (b) x/H=4

(c) x/H=5.8 (d) x/H=13.7

*Secondary flow streamlines in transverse planes of $\mathcal{R}2$ diffuser. The blue line indicates the location of separation surface.*

- Limiting streamlines in $\mathcal{R}2$ and $\mathcal{R}2.5$ are identical, but their secondary flow in the diffuser develop differently.
- The vortices from both walls interact downstream.

# Large Eddy Simulations

- Germano's dynamic Smagorinsky model is used. No wall functions and near-wall damping are needed as local effects are captured in dynamic constant $C_s$.
- Results validated with DNS and separation in diffuser series predicted.
- The averaged Strain and Vorticity fields were used to analyse the fidelity of various analytical stress models.

*Flow variables along baseline diffuser midplane z/B=0.5*

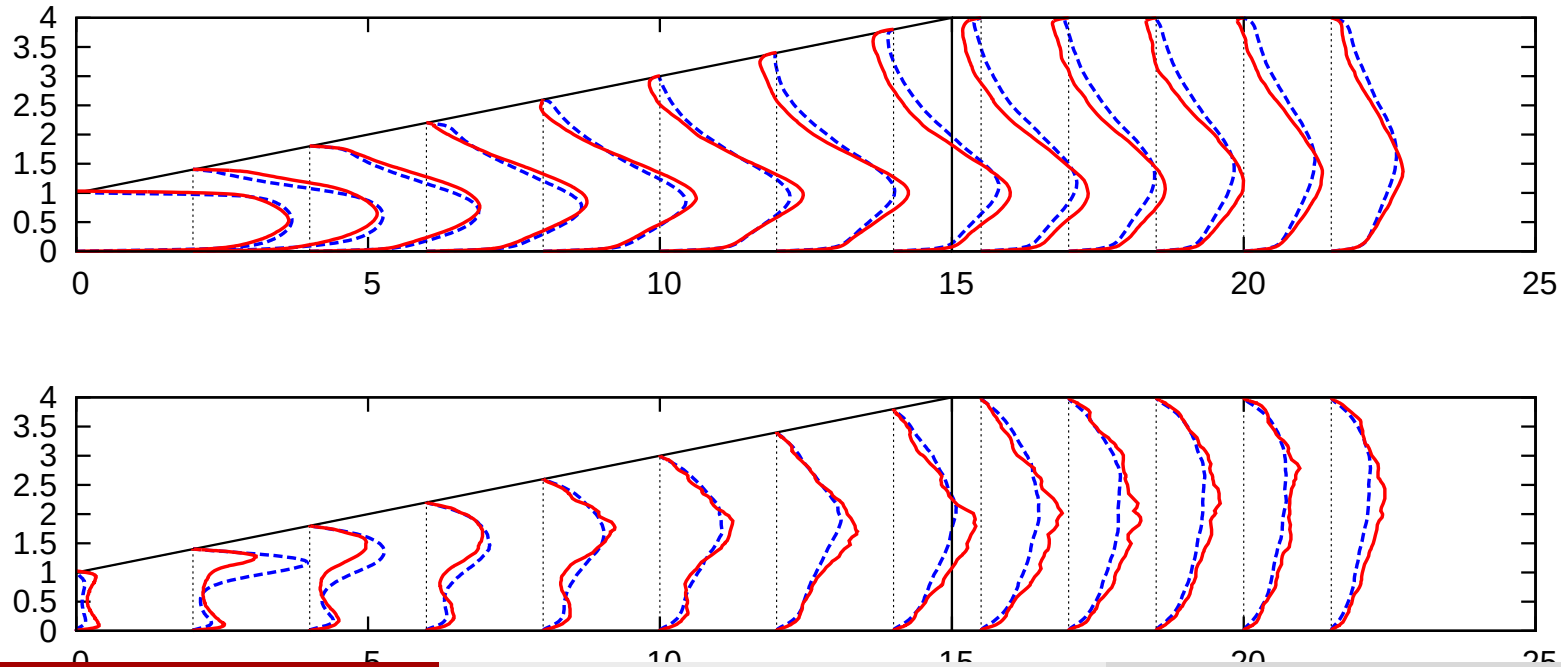

# LES Quality metrics

- A finer grid was used for LES ($477 \times 61 \times 101$) of 3M cells.
- The grid is $4^3$ times smaller that DNS grid used by Ohlsson et al(2010).
- Near-wall resolution is $\Delta y_+ = 2$, $\Delta x_+ = 90$ and $\Delta z_+ = 10$
- Solution quality checks were performed to ensure accuracy of results.
  - 95% of the TKE is resolved
  - The relative SGS index is about 1 in the domain.

$$\frac{k_{res}}{k_{tot}} = \frac{k_{res}}{k_{res}+k_{sgs}+|k_{num}|}$$

$$LES\_IQ_\nu = \frac{1}{1+\alpha_\nu\left(\frac{\overline{\nu}_{eff}}{\nu}\right)^n}$$

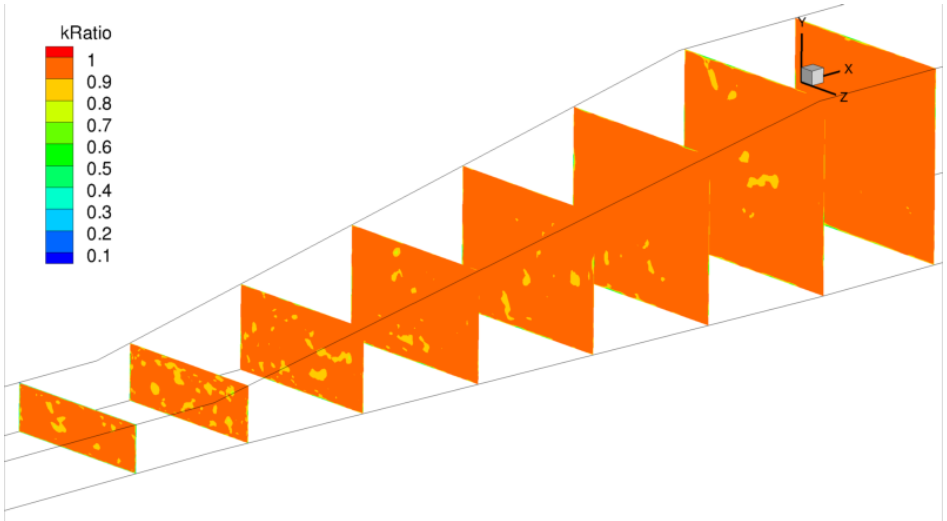


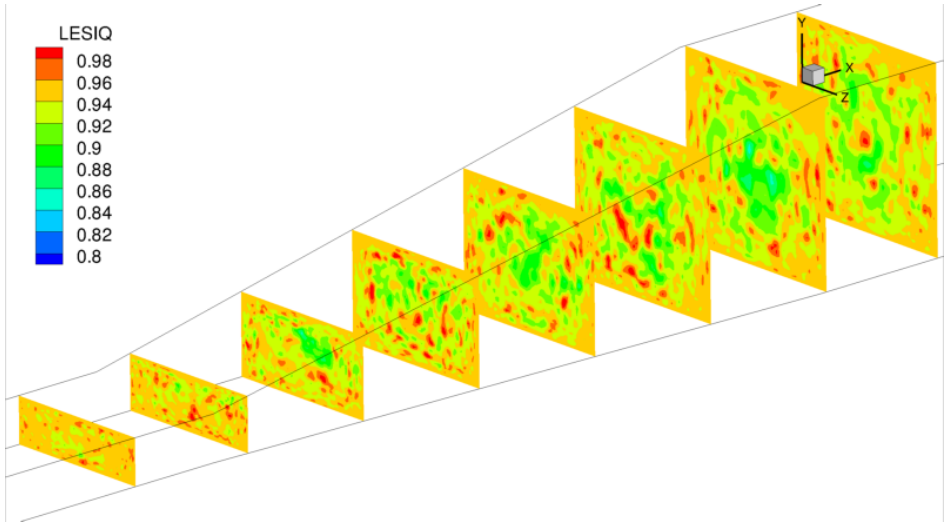

# LES Resolution

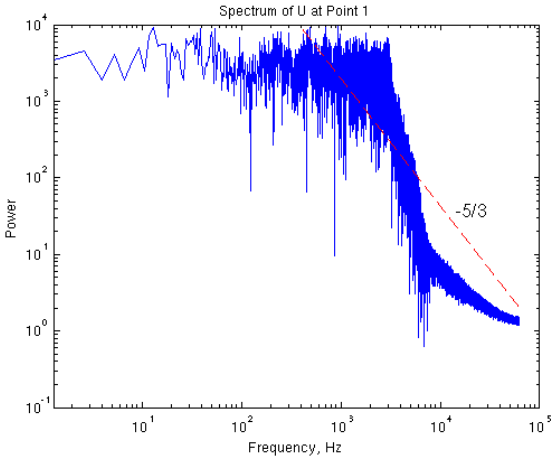


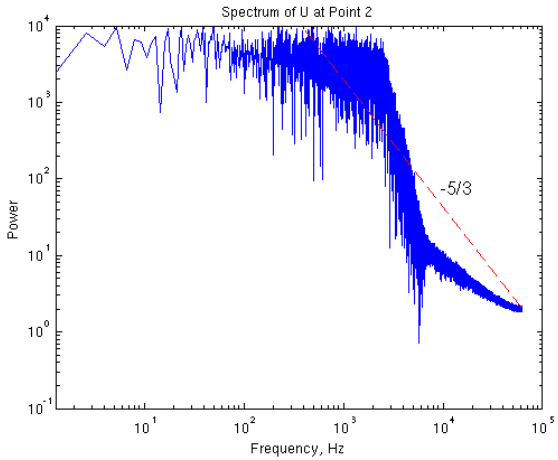


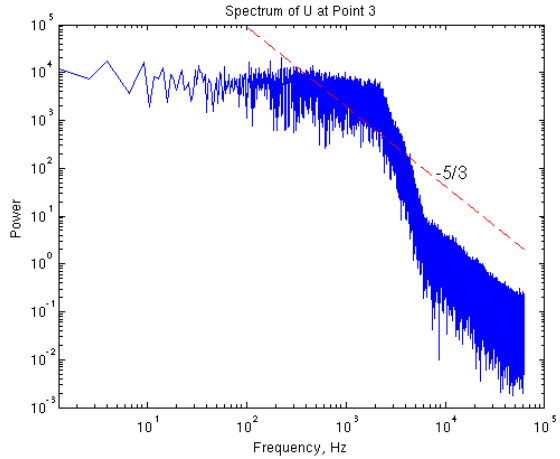


- The cut-off frequency is $3 \times 10^4$ Hz, based on grid size.
- The simulation was performed over 75 Flow-throughs for statistical convergence of flow mean and Reynolds stresses.
- LES resolve a frequency spectrum of 5 orders width (DES resolved 3 orders).
- The slope of inertial range does not follow -5/3 exactly, due to the low Reynolds number and non-homogenity of flow.

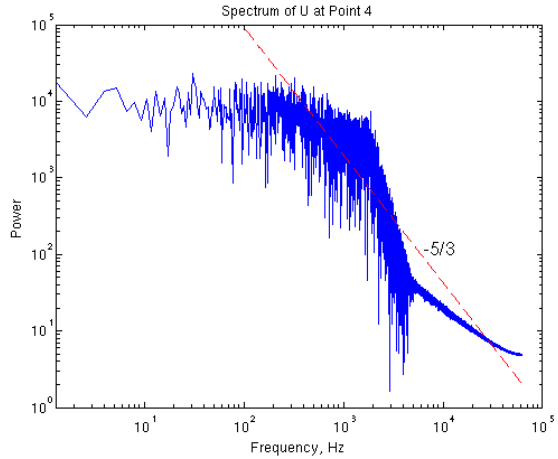

# LES Verification

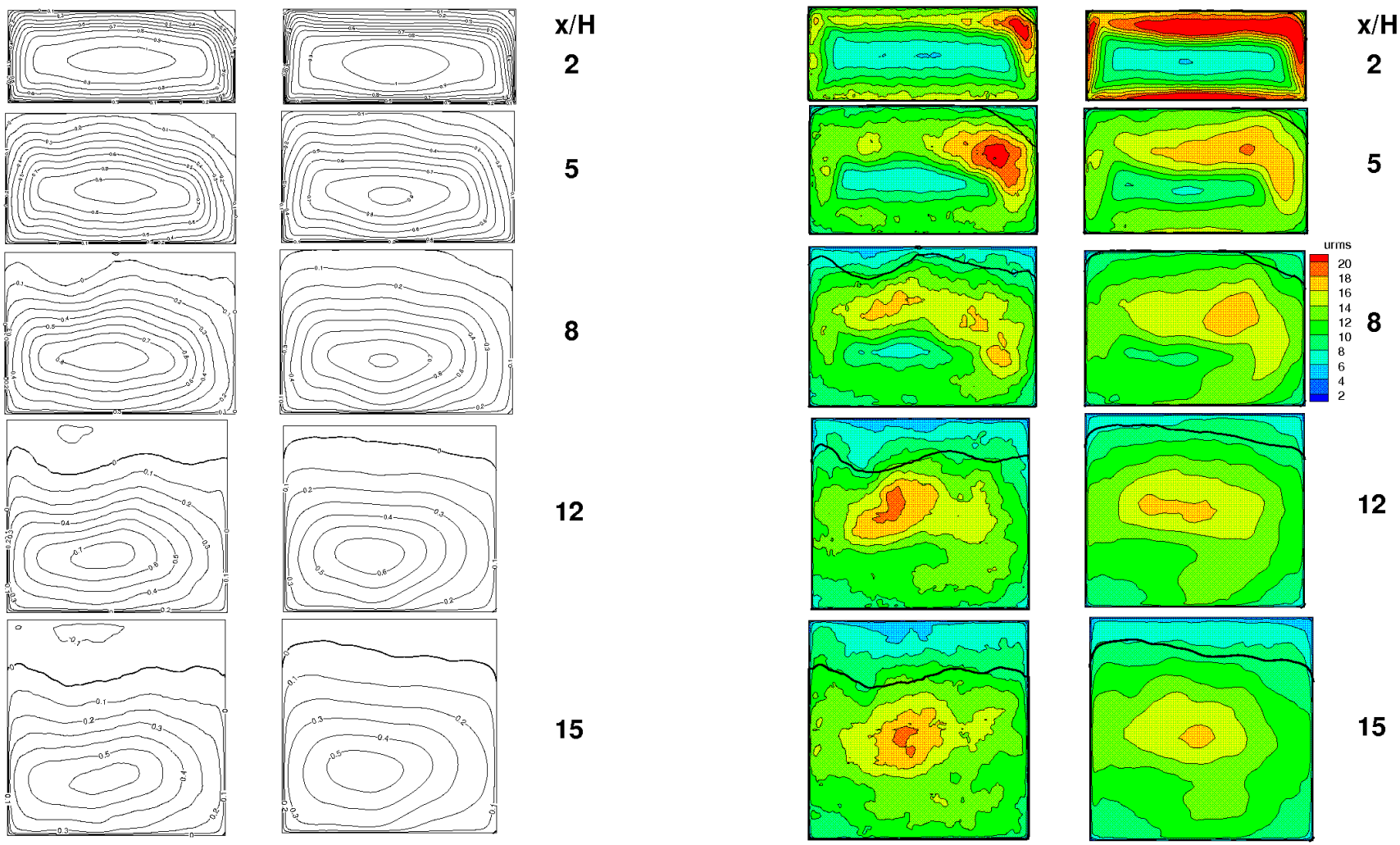


*Contour lines of mean streamwise $\overline{U}$ and $u_{rms}/U_{bulk}$ velocity at transverse planes. DNS is to left and LES on the right. Zero velocity line is bold.*

# Wall pressure

- Accurately predicts the rapid rise of $C_p$ near the inlet of diffuser followed by a gradual reduction in the pressure gradient until the trend becomes linear at about x/L=0.7
- The separation spreads over the top at x/L=0.53, where the change in slope is noticed.

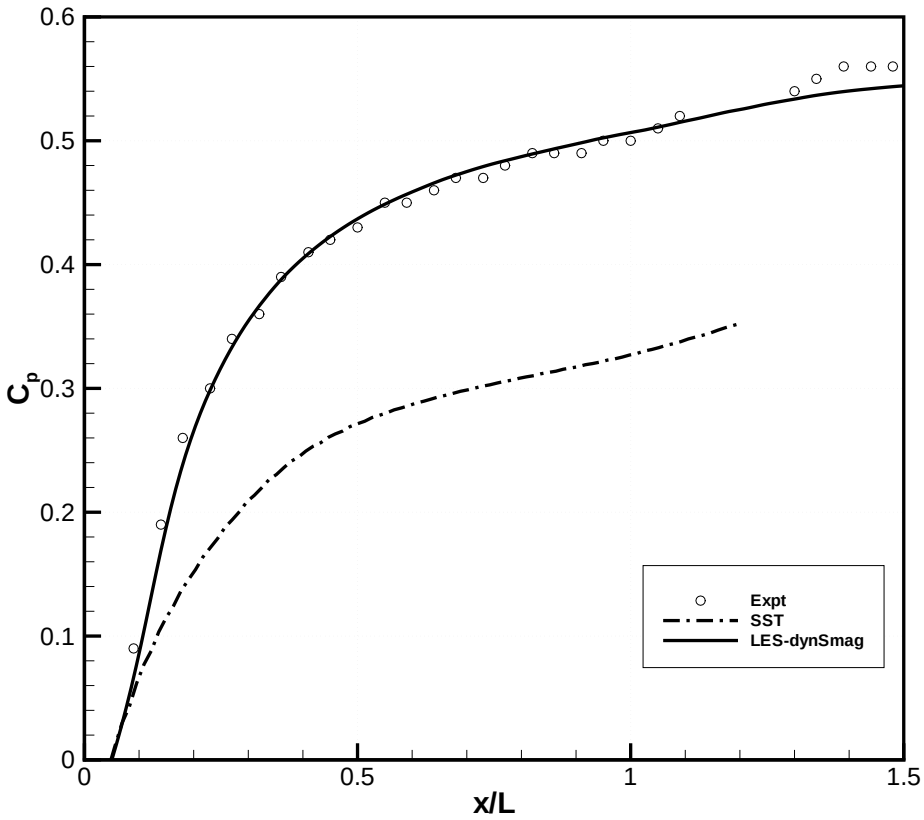


*Coefficient of pressure* $\left(C_p = \frac{p - p_{ref}}{0.5\rho U_{bulk}^2}\right)$ *variation along the bottom wall of baseline diffuser predicted by LES, x/L is the non-dimensional diffuser length.*

# Diffuser series

- The separation surface switches to side wall at about $\text{Æ}3$
- $C_p$ along diffuser is same for $\text{Æ} \geq 2$, with maximum pressure recovery of 80%.

*Secondary flow indicate the same set of corner vortices across Æseries*

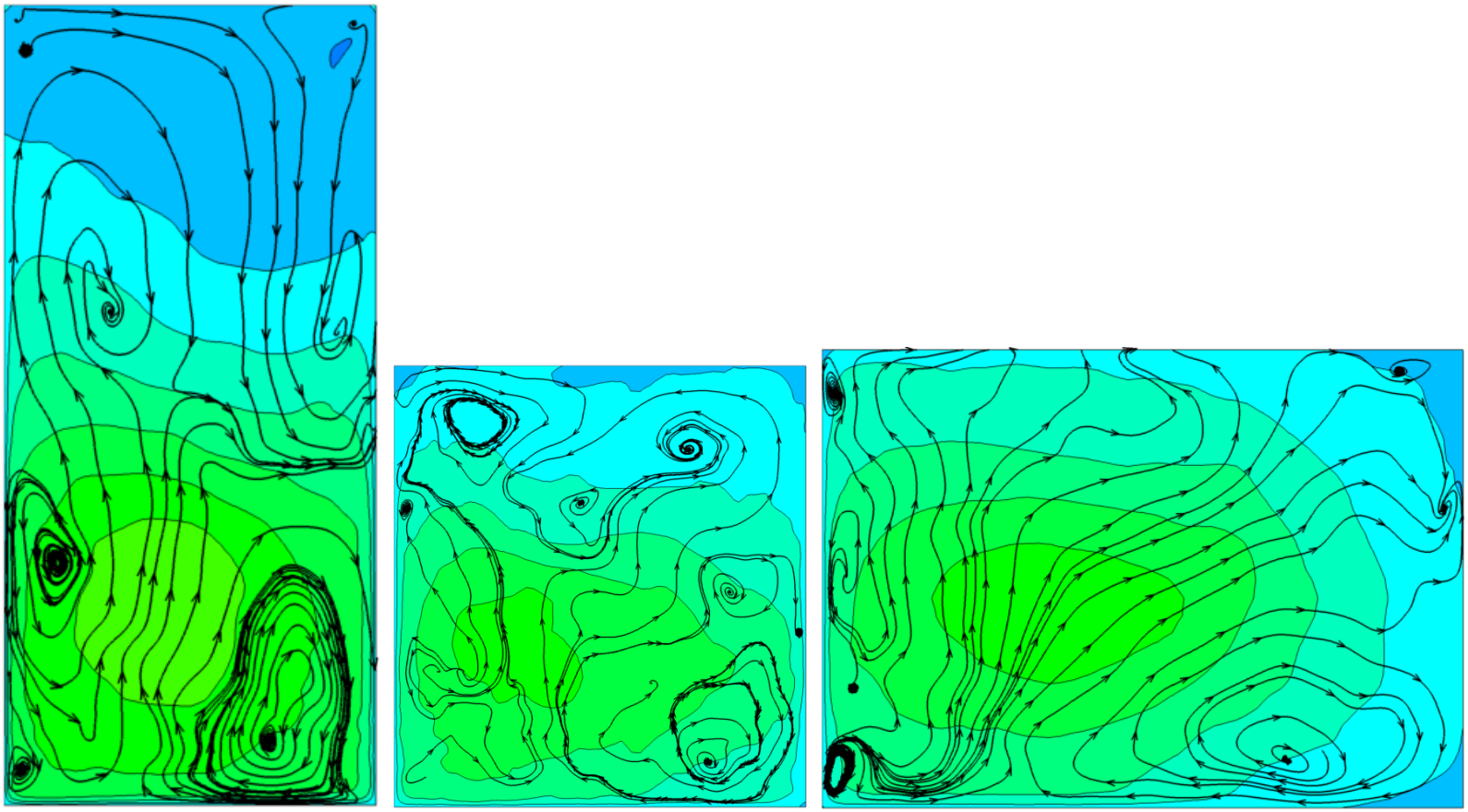

(e) $\text{Æ}1$ (f) $\text{Æ}2$ (g) $\text{Æ}3$

# Outline

# Modeling for separated flows

- Turbulent separation is characterized by increased strain rates and high Production-to-dissipation($\mathcal{P}/\varepsilon$) ratio.
- In 2–D separation,
  - At moderate strain rates, most LEVM predict accurately.
  - At high strain rates, $\mathcal{P}/\varepsilon \gg 1$ which makes $\frac{-\overline{uv}}{k} > \sqrt{C_\mu}(= 0.3)$.
  - Most EVM's are linear in strain, i.e. $a_{ij} = -2\nu_T S_{ij}$, due to the Boussinesq assumption
- In 3–D separation,
  - Normal Stress anisotropy is critical, as boundary layers interact causing normal stress difference($\overline{u^2} - \overline{v^2}$) and secondary shear stresses($\overline{vw}$).
  - Reynolds stress models (RSM) account for anisotropy implicitly, while the effect is modeled in Non-linear EVM's.
  - Anisotropy is $a_{ij} \equiv \frac{\overline{u_i u_j}}{k} - \frac{2}{3}\delta_{ij}$

# Sensitizing $C_\mu$

- $C_\mu$=0.09 is calibrated for 2–D parallel shear.
- Models need be sensitized to 3–D separation by making $C_\mu$ to be dependent on parameters whose,
  - Values vanish in 2–D flows
  - Show proper sensitivity to real physics of separation
  - Computationally inexpensive
  - have Galilean invariance property
- This varies the eddy-viscosity and hence production,$\mathcal{P}/\varepsilon = C_\mu \frac{II_S}{2}$; $II_s = S_{ij}S_{ij}$

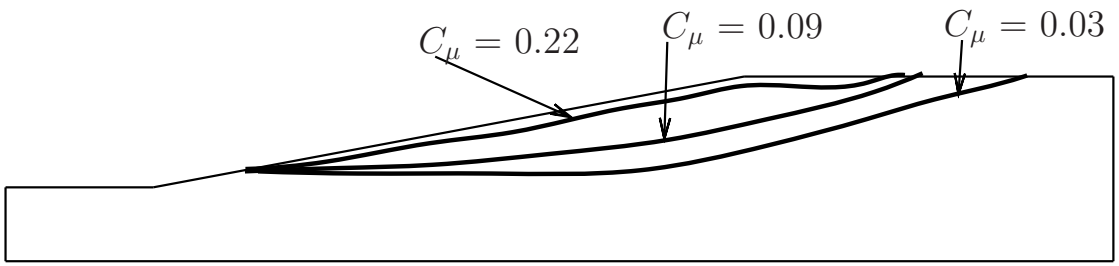


*Sensitivity of 2–D Obi's diffuser separation to varying $C_\mu$*

- The mean velocity gradient tensor is known to resolve the turbulence dynamics. Parameters as Eigen values of VG, $U \cdot (\nabla \times U)$, WALE term were tested, but to no benefit.

# Importance of Anisotropy

- Anisotropy invariant map using DNS data of Ohlsson et al(2010) indicate the bulk of flow to be close to be close to isotropy.
- Maximum anisotropy is at the inlet. The stress tensor until x/B=0.5 is similar to than in 2-D channel, with dominant diagonal terms. The flow undergoes axisymmetric expansion.
- Downstream x/H $>$ 12, the anisotropy undergoes an axisymmetric contraction. This switch happens as the separation spreads over top wall.

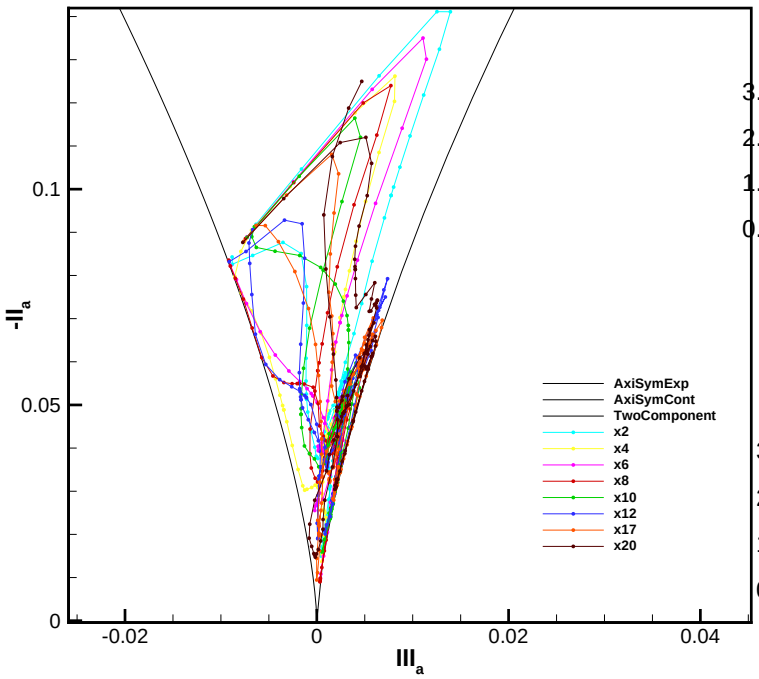


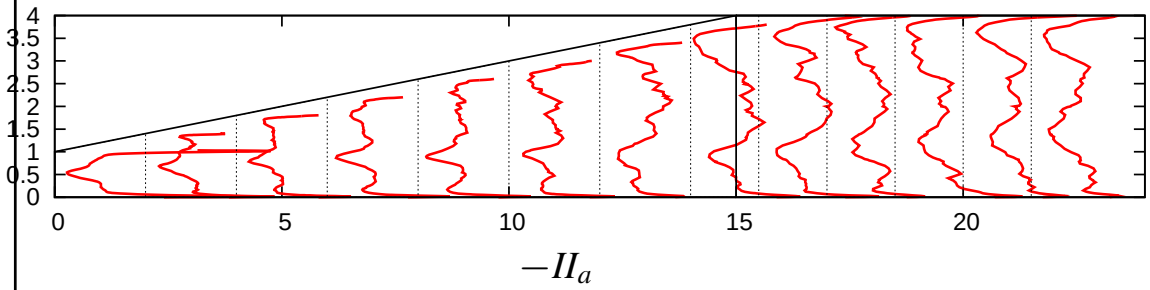


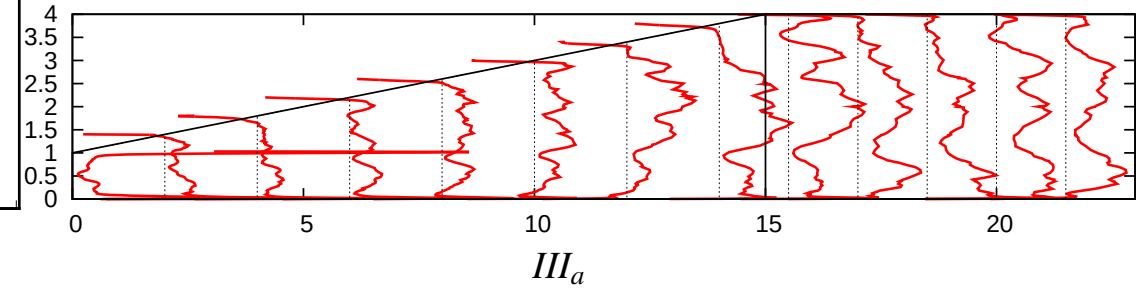

# Anisotropy-resolving models

- In complex strained flows as 3D separation, anisotropy is caused due to lateral straining, streamline curvature, secondary flow of second kind, and transverse pressure gradients.
- Solution to RSM is direct way to solve for evolution of anisotropy.

$$K\frac{\mathcal{D}a_{ij}}{\mathcal{D}t} - \text{Diff}_{ij}^{(a)} = -\frac{\overline{u_i u_j}}{K}(\mathcal{P}-\varepsilon) + \mathcal{P}_{ij} - \varepsilon_{ij} + \Pi_{ij}$$

- Considering 'moving equilibrium' the algebraic RSM can be derived by neglecting $\text{Diff}_{ij}^{(a)}$ and considering a 'moving eqiulibrium', i.e. $\frac{\mathcal{D}}{\mathcal{D}t}\left(\frac{\overline{u_i u_j}}{K}\right) = 0$, which implies $\mathcal{D}_t a_{ij} = 0$. The ARSM is;

$$\frac{\overline{u_i u_j}}{K}(\mathcal{P}-\varepsilon) = \mathcal{P}_{ij} - \varepsilon_{ij} + \Pi_{ij}$$

- ARSM are numerically stiff and non-linear.
- For closure, models are needed for pressure-strain tensor $\Pi_{ij}$ and dissipation $\varepsilon_{ij}$. The later is modeled assuming isotropy and solving an equation for $\varepsilon$.
- $\Pi_{ij}$ model of LRR predicts 3-D diffuser separation accurately than quadratic SSG model.

# Explicit Algebraic Reynolds Stress Model

- Using Cayley-Hamilton theorem $a_{ij}$ can be expressed consistently as a 5-order polynomial $a_{ij} = \mathcal{F}_{ij}(S_{ij}, \Omega_{ij})$
- Substituting this in the ARSM gives the simplified Generalized model equation;

$$\underbrace{\left(c_1 - 1 + \frac{\mathcal{P}}{\varepsilon}\right)}_{N}\mathbf{a} = -\frac{8}{15}\mathbf{S} + \frac{7c_2+1}{11}(\mathbf{a\Omega} - \mathbf{\Omega a}) - \frac{5-9c_2}{11}(\mathbf{aS} + \mathbf{Sa} - \frac{2}{3}\{\mathbf{aS}\}\mathbf{I})$$

- The EARSM has been attractive as they can be derived from the first principles of tensor consistency and assumptions are clear. Pros and Cons are;
  - \+ Accounts for normal stress anisotropy
  - \+ For rotating flows, material frame difference can be included by correcting $\mathbf{\Omega}$
  - \- Streamline curvature and Coriolis contributions need to be included via. $\mathbf{\Omega}$
  - \- only accurate for equilibrium flows
  - \- Anisotropy is only sustained by local velocity gradients.
  - \- Dynamics of stress anisotropy not included.

# EARSM-Further simplifications

- In 2–D, anisotropy tensor only depends on $II_S, II_\Omega$, where in 3–D it depends on 4 invariants.
- The solution to $\mathcal{P}/\varepsilon$ is a $N^3$ polynomial. This has been used in the model as the difference with $N^6$ estimate is only 4%
- The deviation of $IV = \{\boldsymbol{S\Omega^2}\}$ and $V = \{\boldsymbol{S^2\Omega^2}\}$ from 2–D invariants is used to qualitatively assess the 3–D nature of anisotropy.

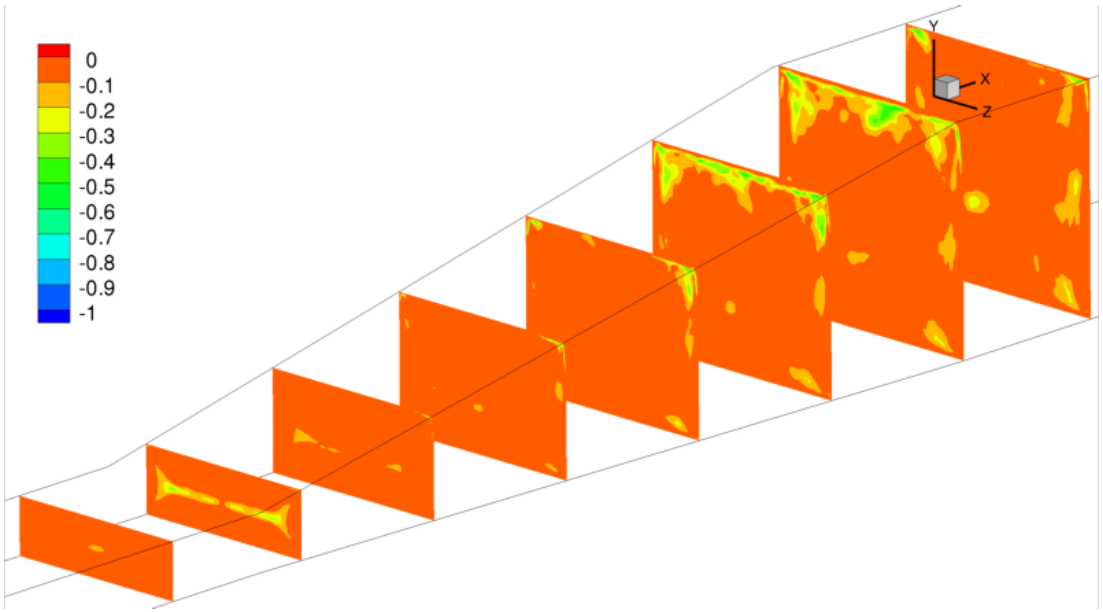


*Visualization of* $\left(V - \frac{II_S II_\Omega}{2}\right)$ *from LES. Regions of 0 have no 3D influence on anisotropy and regions of -1 have full 3D influence*

# Implementation

- The turbulence length scale is determined by $k-\omega$ formulation of Menter (2009).
- A 2nd-order scheme for divergence terms, as the accuracy of anisotropy is dependent on VG evaluation.
- Discretization of dissipative term is performed as $\partial_j \left[\nu \partial_j U_i - \overline{u_j u_i}\right]$ rather than $\partial_j \left[\nu \partial_j U_i\right] - \partial_j \left[\overline{u_j u_i}\right]$. The former is less stiff.
- Gauss-Seidel smoother is used. All divergence terms are upwind and Laplacian terms are 2nd-order accurate.
- This implementation is called the 'Baseline EARSM', BEARSM.

# Baseline diffuser - BEARSM

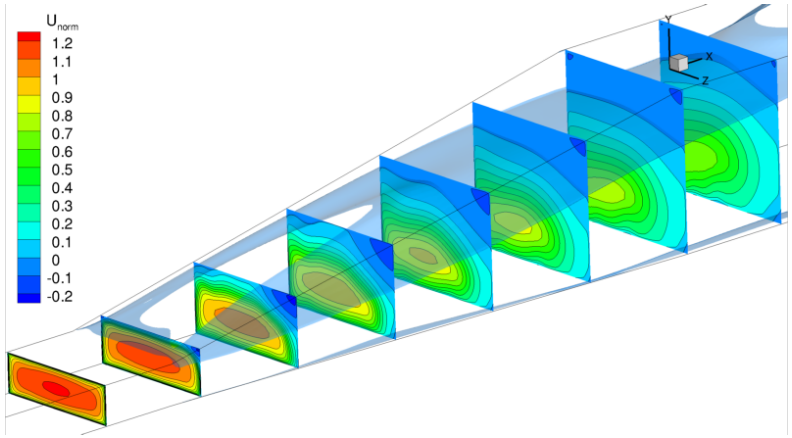


*The BEARSM predicts separation on the top side, while the LEVM predicts along the side wall.*

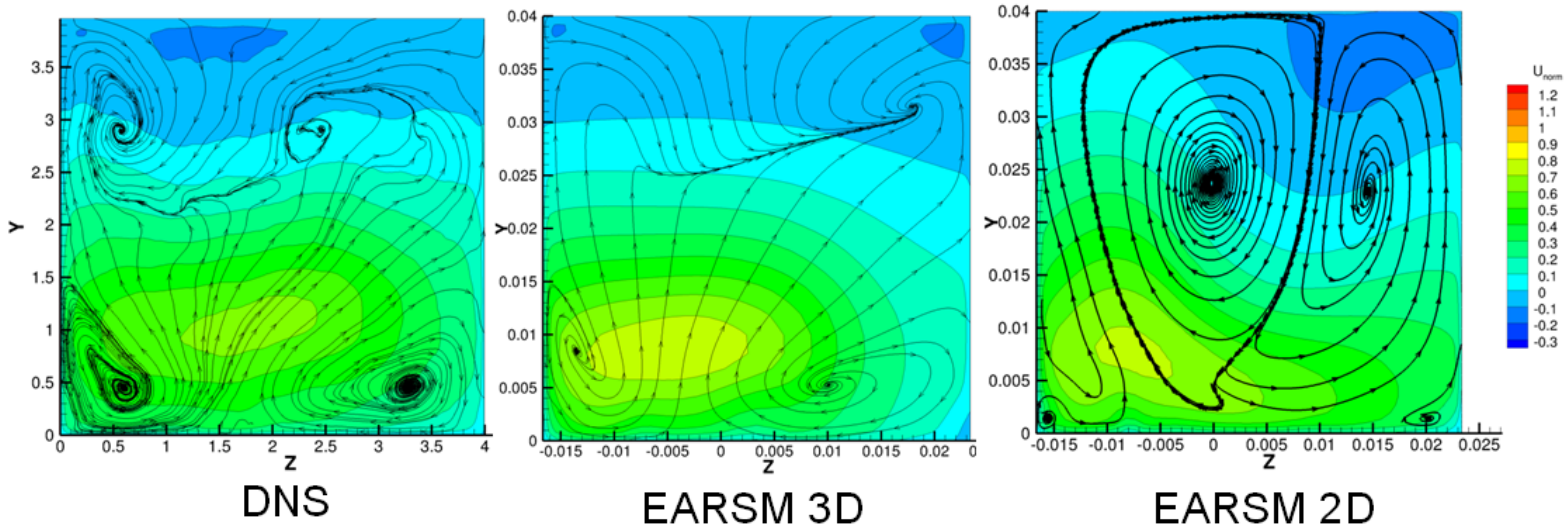


*Secondary flow at the diffuser exit x/H=15. The 2–D and 3–D formulation of anisotropy are compared.*

# Baseline diffuser - BEARSM

- Separation volumes by the model is higher than DNS, however it spreads over top at same x/H=6
- The model sustains a larger core flow velocity, mainly due to absence of relaxation effects on eddy-viscosity
- Secondary flow vortices are accurately resolved

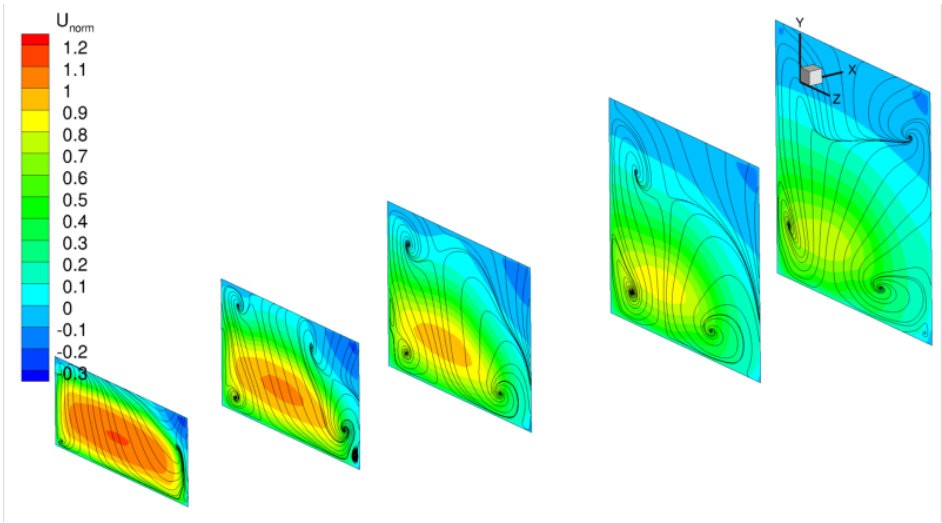


*BEARSM*

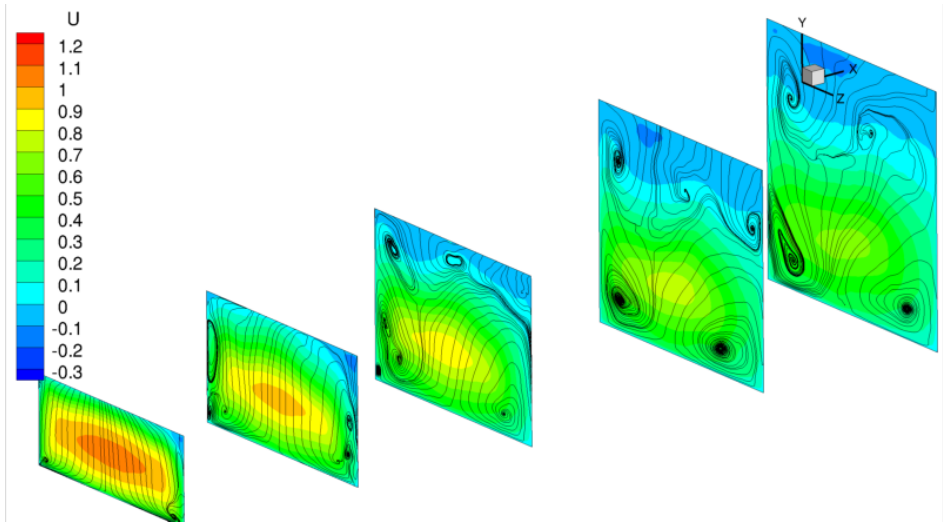


*DNS*

# Diffuser series - BEARSM

- Qualitatively, the model predicts transition at $\AA 3$, same as LES.
- A larger separation surface is predicted by model in the family of diffusers.
- The EARSM is able to sustain a higher shear stress distribution compared to LES, as the algebraic stress approximation leads to high strain asymptotic limit.

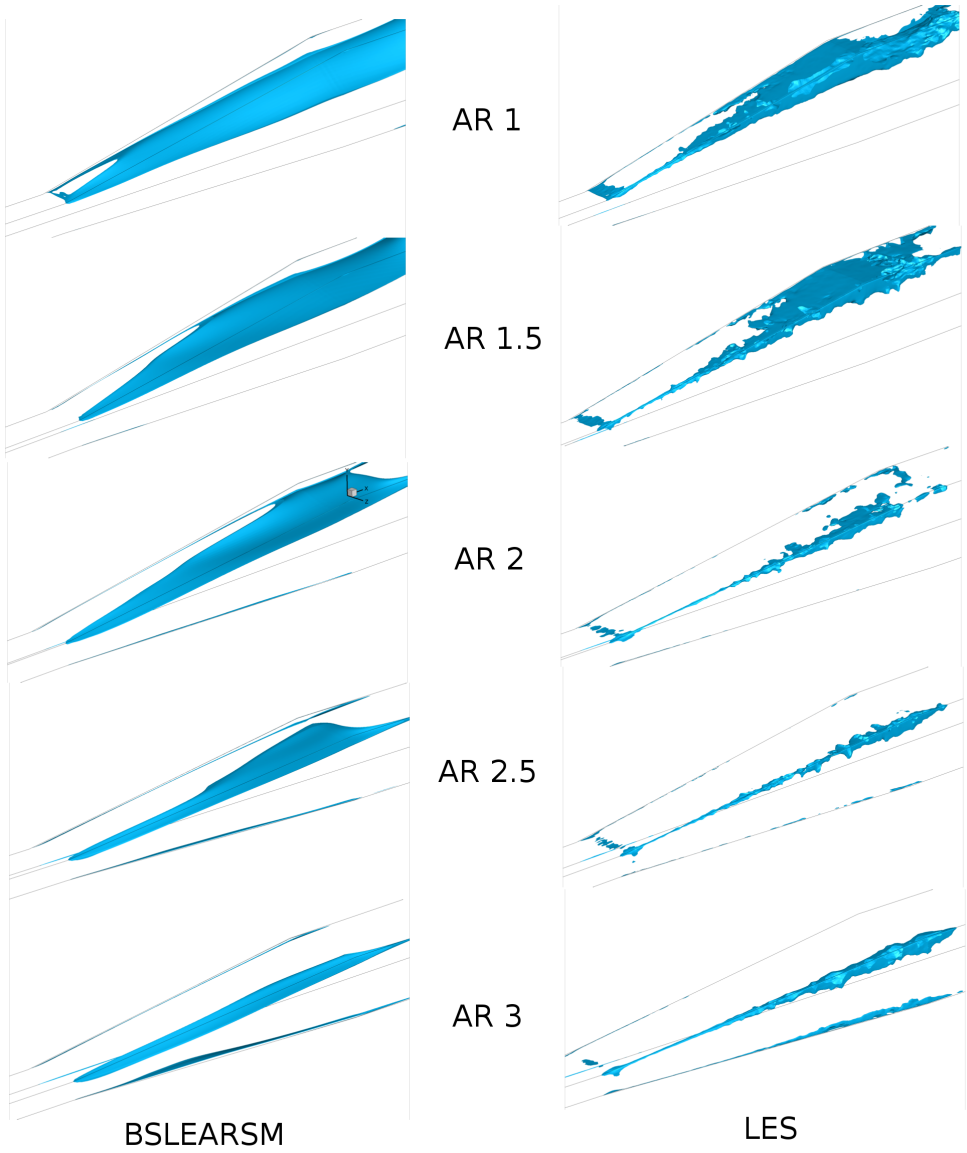

# $C_p$ in Diffuser series - BEARSM

- The $C_p$ distribution has the same trend of LES, however the pressure recovery is lower.
- The inflection point in $C_p$ curve is located at x/L=0.4, similar to LES, as the spreading of separation on top wall is accurately predicted.

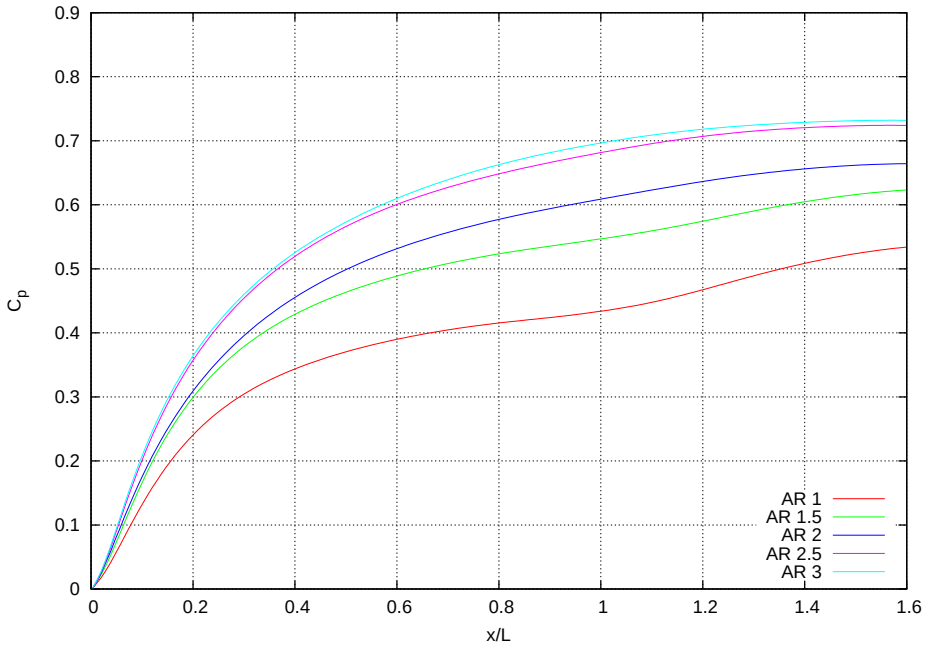


*BEARSM*

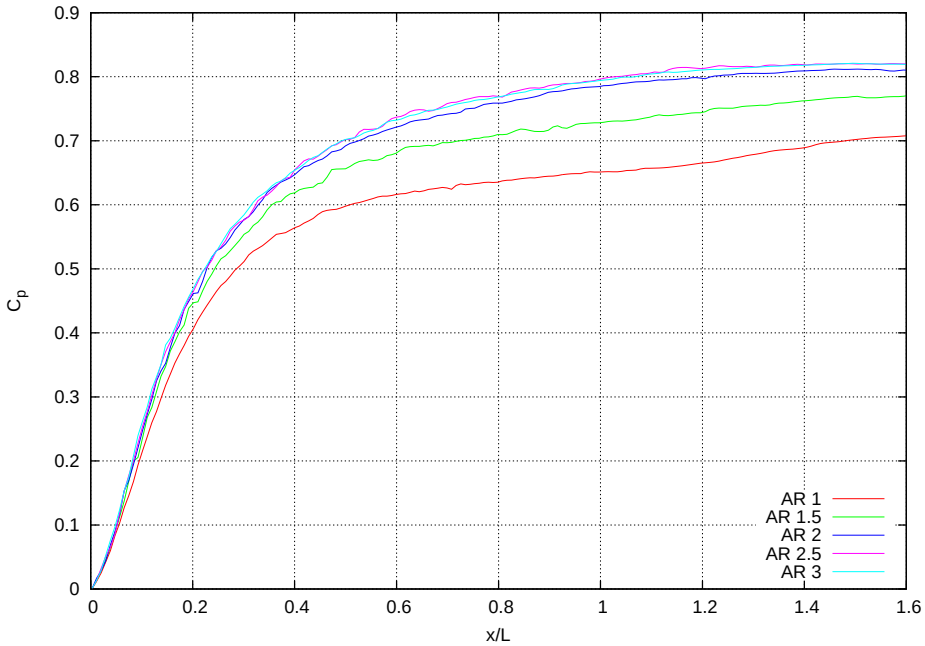


*DNS*

# Generalized quasi-linear EARSM

- The Generalized ARSM does not consider $c_2 = 5/9$, and solves for;
  $N\mathbf{a} = -A_1\mathbf{S} + (\mathbf{a\Omega} - \mathbf{\Omega a}) - A_2(\mathbf{aS} + \mathbf{Sa} - \frac{2}{3}\{\mathbf{aS}\});\ N = A_3 + A_4\frac{\mathcal{P}}{\varepsilon}$
- The coefficients for standard $\Pi^r_{ij}$ models are:

| | $A_1$ | $A_2$ | $A_3$ | $A_4$ |
|---|---|---|---|---|
| EARSM-WJ2000($c_1$=1.8, $c_2$=5/9) | 1.2 | 0 | 1.8 | 2.25 |
| Original LRR($c_1$=1.5, $c_2$=0.4) | 1.54 | 0.37 | 1.45 | 2.89 |
| Linearized SSG | 1.22 | 0.47 | 0.88 | 2.37 |

- The generalized model predict diffuser separation the same as the RSM. The error originates from the pressure-strain model $\Pi^r_{ij}$ for rapid part.

*original LRR*

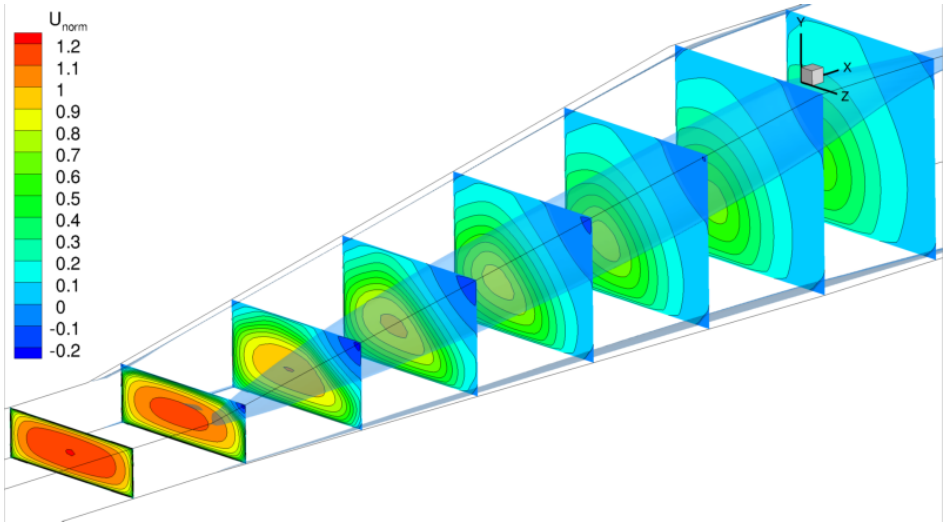


*linearized SSG*

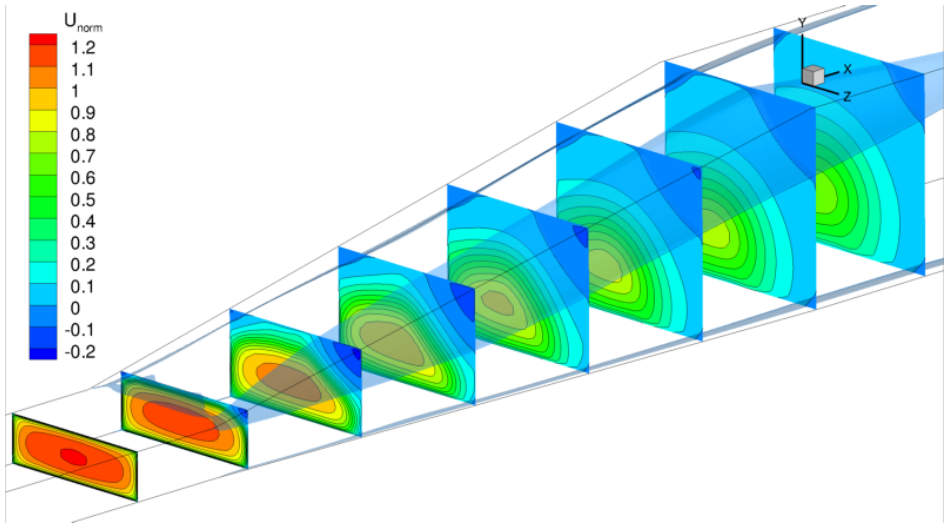

# Square Duct

Huser & Biringer (1993) data has been used to quantify the predictability of secondary flow of 2nd kind. Though the anisotropies are fairly accurate, the magnitudes of Turbulent kinetic energy are lower than DNS. As the secondary flow is only driven by turbulent anisotropy, this leads to a weaker secondary flow.

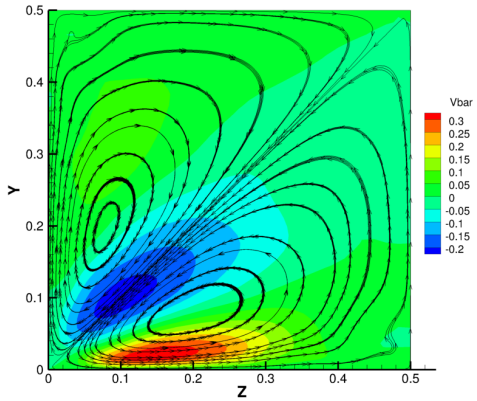


DNS

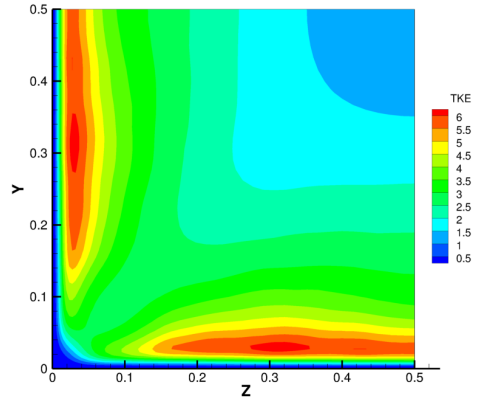


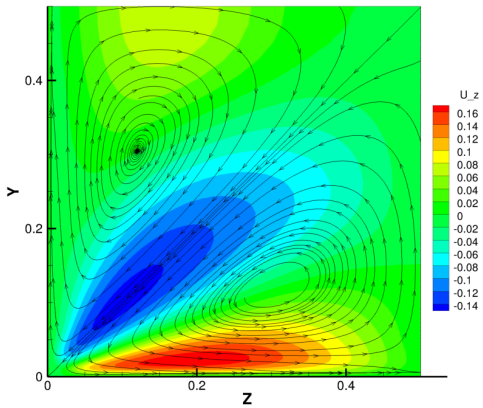


EARSM

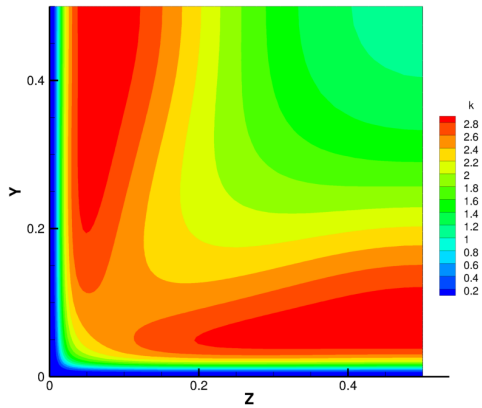

# Homogeneous shear flow – RSM

- In this simplified flow, a direct solution to the RSE can be sought. The modeling assumptions boil down to coefficients of pressure-strain term.
- The experimentally predicted anisotropy is: $\begin{pmatrix} 0.36 & -0.32 & 0 \\ -0.32 & -0.22 & 0 \\ 0 & 0 & -0.14 \end{pmatrix}$
- Anisotropy by LRR-WJ2000 $\begin{pmatrix} 0.29 & -0.3 & 0 \\ -0.3 & -0.29 & 0 \\ 0 & 0 & 0 \end{pmatrix}$ and Original LRR $\begin{pmatrix} 0.29 & -0.37 & 0 \\ -0.37 & -0.23 & 0 \\ 0 & 0 & -0.0641 \end{pmatrix}$
- Calibrated LRR has $a_{12}$ and $a_{11}$ matched and the $C_{1,2,3}$ evaluated.

| | $C_1$ | $C_2$ | $C_3$ |
|---|---|---|---|
| LRR (WJ2000) | 1.8 | 0.77 | 0.22 |
| Original LRR | 1.8 | 0.763 | 0.109 |
| Calibrated LRR | 1.302 | 0.7739 | 0.189 |
| Linearized SSG | $1.7+0.9\frac{\mathcal{P}}{\varepsilon}$ | 0.4125 | 0.2125 |

- A diffuser simulation with EARSM using these coefficients predicted separation accurately (similar to WJ2000), an improvement over Original LRR, however is computationally intensive.

# Comparison of $C_p$ predictions

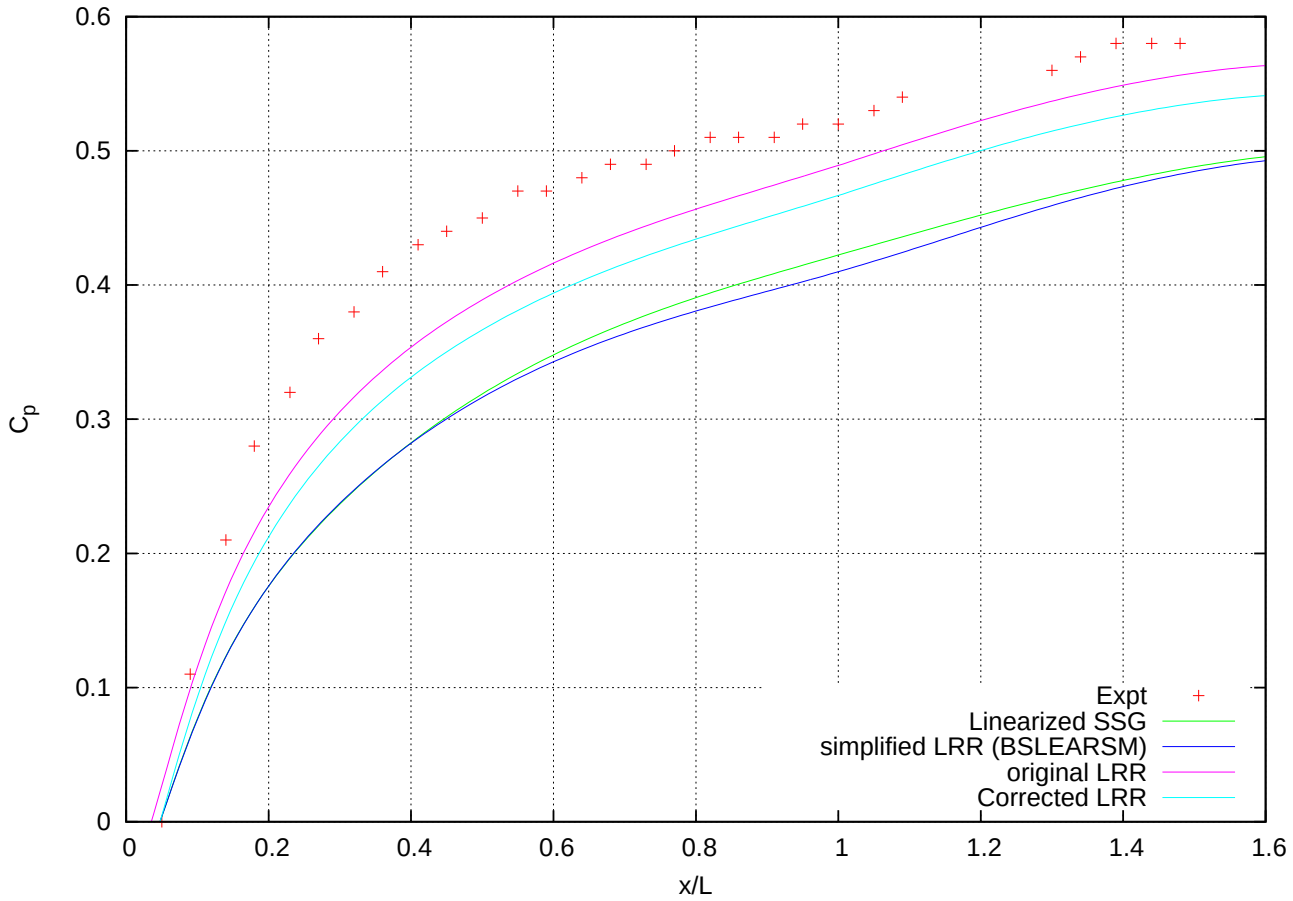


Figure: Wall $C_p$ predicted by different Generalized EARSM models

# Diffusion-corrected EARSM

- The "moving equilibrium" assumption considers asymptotic state, or high strain limit $\mathbf{S}K/\varepsilon$. Due to this the EARSM will be incorrect in regions of mild strain as in the core of flow, where $\mathcal{P}/\varepsilon$ is low.
- The correction modifies N in ARSM as: $c_1^{'} = \frac{9}{4}\left(C_1 - 1 - \frac{C_D}{\varepsilon}\frac{\partial}{\partial x}(\nu\frac{\partial}{\partial x}K)\right)$
- The modified term does not alter the separation surface, however the secondary flow resolves the top vortices. This is not major as secondary flow is only 1% of $U_{bulk}$.

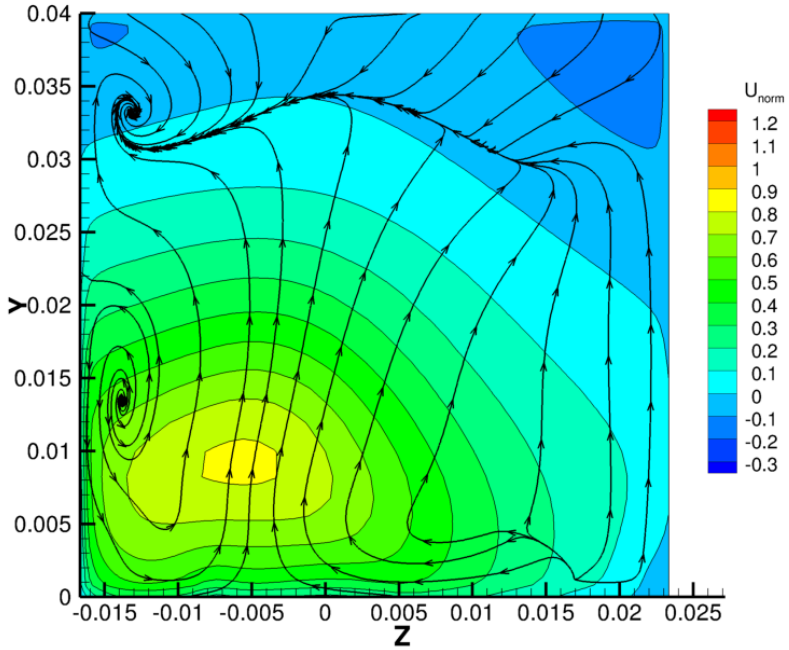

# Further Modeling Refinements – "Future Work"

Further scope for improvement of predictive accuracy of EARSM exists. They are;

1. *Pressure-strain modeling* As pointed earlier, this is the root of many of the errors observed. The model constants could be made functions of strain field invariants (as in SSG)
2. *Length scale equation* For better near-wall prediction. As it is critical to separated flows.
3. *Adjustment to low Strain rate* This improvement proposed by Taulbee (1992) accounts for transport of second invariant of strain $\frac{\mathcal{D}}{\mathcal{D}t}\left(\sqrt{II_S}\right)$. Hence non-local effects affect anisotropy.
4. *Stress-strain lag* The model developed by Revell(2006) accounts for lag by solving for an additional transport equation for $\frac{\mathcal{D}}{\mathcal{D}t}\left(\frac{\mathcal{P}}{\varepsilon}\right)$ and uses it to limit $\nu_T$ and calculate turbulence production $\widetilde{P}_k(=-k\frac{\mathcal{P}}{\varepsilon})$. Would benefit separation with mean flow unsteadiness.
5. *Curvature correction* The Spalart-Shur correction to vorticity did not alter the separation. The WJ (2002) curvature correction has not been tested on the diffuser.

# Outline

# Conclusions

- The diffuser flow has vortices that originate from singular points on wall and interact downstream.
- The pattern of the wall stress lines remain same though the diffuser series, the singular points moved closer to inlet as $\mathcal{R}$increases.
- Turbulence Anisotropy is critical in 3-D flow separation
  - The reverse flow undergoes axisymmetric contraction, while anisotropy in most of the other flow undergoes axisymmetric expansion
  - Three-dimensionality of velocity gradient field has a high effect on accurate prediction of anisotropy
- The DES model is found to be quantitatively incorrect for diffuser flows in predicting wall pressure.
- The Anisotropy-resolving model EARSM qualitatively predicts mean separation accurately, however the second-moments are inaccurate.
- Refinements to the EARSM needs improved pressure-strain modeling.

# Conclusions

- The diffuser flow has vortices that originate from singular points on wall and interact downstream.
- The pattern of the wall stress lines remain same though the diffuser series, the singular points moved closer to inlet as $\mathcal{R}$increases.
- Turbulence Anisotropy is critical in 3-D flow separation
  - The reverse flow undergoes axisymmetric contraction, while anisotropy in most of the other flow undergoes axisymmetric expansion
  - Three-dimensionality of velocity gradient field has a high effect on accurate prediction of anisotropy
- The DES model is found to be quantitatively incorrect for diffuser flows in predicting wall pressure.
- The Anisotropy-resolving model EARSM qualitatively predicts mean separation accurately, however the second-moments are inaccurate.
- Refinements to the EARSM needs improved pressure-strain modeling.

# Conclusions

- The diffuser flow has vortices that originate from singular points on wall and interact downstream.
- The pattern of the wall stress lines remain same though the diffuser series, the singular points moved closer to inlet as $\mathcal{R}$increases.
- Turbulence Anisotropy is critical in 3-D flow separation
  - The reverse flow undergoes axisymmetric contraction, while anisotropy in most of the other flow undergoes axisymmetric expansion
  - Three-dimensionality of velocity gradient field has a high effect on accurate prediction of anisotropy
- The DES model is found to be quantitatively incorrect for diffuser flows in predicting wall pressure.
- The Anisotropy-resolving model EARSM qualitatively predicts mean separation accurately, however the second-moments are inaccurate.
- Refinements to the EARSM needs improved pressure-strain modeling.

# Conclusions

- The diffuser flow has vortices that originate from singular points on wall and interact downstream.
- The pattern of the wall stress lines remain same though the diffuser series, the singular points moved closer to inlet as $\mathcal{R}$increases.
- Turbulence Anisotropy is critical in 3-D flow separation
  - The reverse flow undergoes axisymmetric contraction, while anisotropy in most of the other flow undergoes axisymmetric expansion
  - Three-dimensionality of velocity gradient field has a high effect on accurate prediction of anisotropy
- The DES model is found to be quantitatively incorrect for diffuser flows in predicting wall pressure.
- The Anisotropy-resolving model EARSM qualitatively predicts mean separation accurately, however the second-moments are inaccurate.
- Refinements to the EARSM needs improved pressure-strain modeling.

# Conclusions

- The diffuser flow has vortices that originate from singular points on wall and interact downstream.
- The pattern of the wall stress lines remain same though the diffuser series, the singular points moved closer to inlet as $\mathcal{R}$increases.
- Turbulence Anisotropy is critical in 3-D flow separation
  - The reverse flow undergoes axisymmetric contraction, while anisotropy in most of the other flow undergoes axisymmetric expansion
  - Three-dimensionality of velocity gradient field has a high effect on accurate prediction of anisotropy
- The DES model is found to be quantitatively incorrect for diffuser flows in predicting wall pressure.
- The Anisotropy-resolving model EARSM qualitatively predicts mean separation accurately, however the second-moments are inaccurate.
- Refinements to the EARSM needs improved pressure-strain modeling.

# Conclusions

- The diffuser flow has vortices that originate from singular points on wall and interact downstream.
- The pattern of the wall stress lines remain same though the diffuser series, the singular points moved closer to inlet as $\mathcal{R}$increases.
- Turbulence Anisotropy is critical in 3-D flow separation
  - The reverse flow undergoes axisymmetric contraction, while anisotropy in most of the other flow undergoes axisymmetric expansion
  - Three-dimensionality of velocity gradient field has a high effect on accurate prediction of anisotropy
- The DES model is found to be quantitatively incorrect for diffuser flows in predicting wall pressure.
- The Anisotropy-resolving model EARSM qualitatively predicts mean separation accurately, however the second-moments are inaccurate.
- Refinements to the EARSM needs improved pressure-strain modeling.

# Conclusions

- The diffuser flow has vortices that originate from singular points on wall and interact downstream.
- The pattern of the wall stress lines remain same though the diffuser series, the singular points moved closer to inlet as $\mathcal{R}$increases.
- Turbulence Anisotropy is critical in 3-D flow separation
  - The reverse flow undergoes axisymmetric contraction, while anisotropy in most of the other flow undergoes axisymmetric expansion
  - Three-dimensionality of velocity gradient field has a high effect on accurate prediction of anisotropy
- The DES model is found to be quantitatively incorrect for diffuser flows in predicting wall pressure.
- The Anisotropy-resolving model EARSM qualitatively predicts mean separation accurately, however the second-moments are inaccurate.
- Refinements to the EARSM needs improved pressure-strain modeling.

# Outline

The RANS equations are:

$$\partial_t U_i + U_j \partial_j U_i = -\frac{1}{\rho}\partial_i P + \nu \nabla^2 U_i \boldsymbol{-\partial_j \overline{u_j u_i}} \text{ and} \partial_i U_i = 0$$

The transport equation of the Reynolds stress $\overline{u_i u_j}$ is,

$$\overline{U_k}\frac{\partial \overline{u_i u_j}}{\partial x_k} = P_{ij} + T_{ij} + D_{ij} + D_{p,ij} + \Phi_{ij} - \epsilon_{ij}$$

where the left-hand term is convection and the right-hand terms are defined as:

Production: $P_{ij} = -\overline{u_i u_k}\frac{\partial \overline{U_i}}{\partial x_k} - \overline{u_j u_k}\frac{\partial \overline{U_i}}{\partial x_k}$

Turbulent diffusion: $T_{ij} = -\frac{\partial \overline{u_i u_j u_k}}{\partial x_k}$

Viscous diffusion: $D_{ij} = \nu \frac{\partial^2 \overline{u_i u_j}}{\partial x_k^2}$

Pressure diffusion: $D_{p,ij} = -\frac{1}{\rho}\left(\frac{\partial \overline{u_j p}}{\partial x_i} + \frac{\partial \overline{u_i p}}{\partial x_j}\right)$

Pressure strain: $\Phi_{ij} = \overline{\frac{p}{\rho}\left(\frac{\partial u_i}{\partial x_j} + \frac{\partial u_j}{\partial x_i}\right)}$

Dissipation: $\epsilon_{ij} = 2\nu \overline{\frac{\partial u_i}{\partial x_k}\frac{\partial u_j}{\partial x_k}}$

-lower case are fluctuating quantities and upper case the means.

Redistribution tensor:

$$\Pi_{ij} \equiv -\frac{1}{\rho}\left(\overline{u_i \frac{\partial p}{\partial x_j} + u_j \frac{\partial p}{\partial x_i}}\right) = \Phi_{ij} + D_{p,ij}$$

# 2D hump geometry

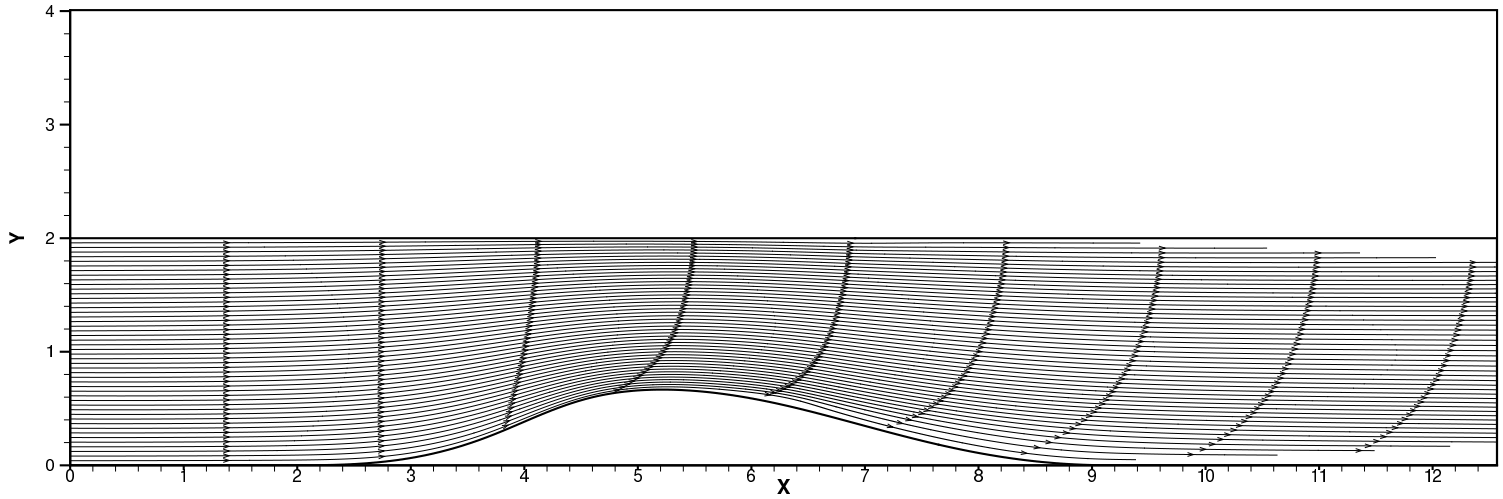


| Hump Geometry | Re($=\frac{U_\infty h_{hump}}{\nu}$) | Simulation | Reference |
|---|---|---|---|
| Goldschmeid hump | 119,674 | LES | You et al. [2006] |
| Convergent-divergent channel | 8,404 | DNS | Marquillie et al. [2008] |
| Periodic hill | 12,714 | LES | Fröhlich et al. [2005] |
| Rounded step | 13,700 | LES | Lardeau et al. [2011] |

Table: 2-D hump geometries studied using highly-resolved simulations. The data sets available using simulation type is indicated

# *a-priori* studies of 2-D separation–Pressure-strain model

- In a 2-D periodic hill separation, the EARSM over predicts separation bubble.
- The pressure-strain models under respond at the high shear(and $\mathcal{P}/\varepsilon$) near start of separation. $\Pi_{ij}$ responds with a lag to the stress.

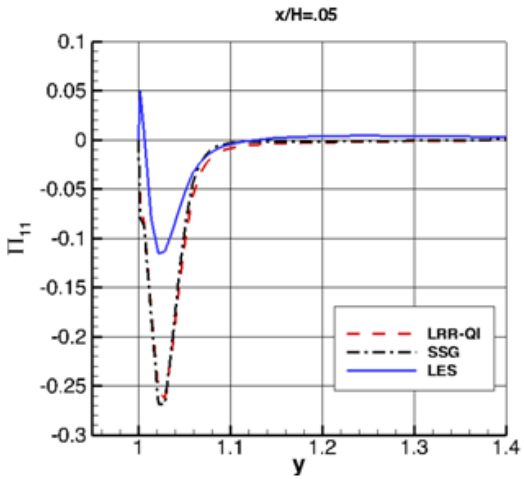


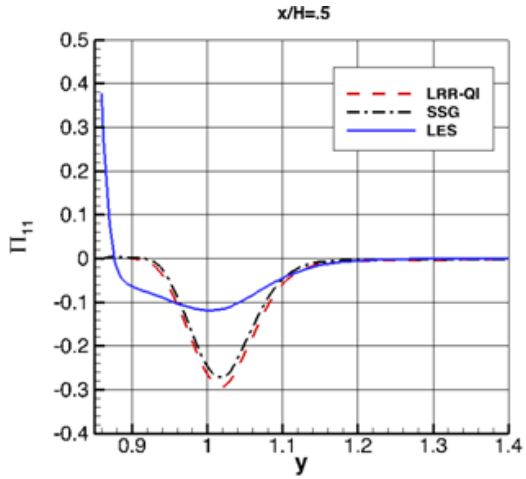


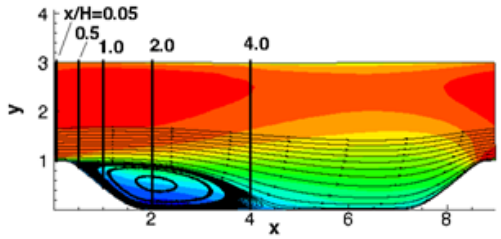


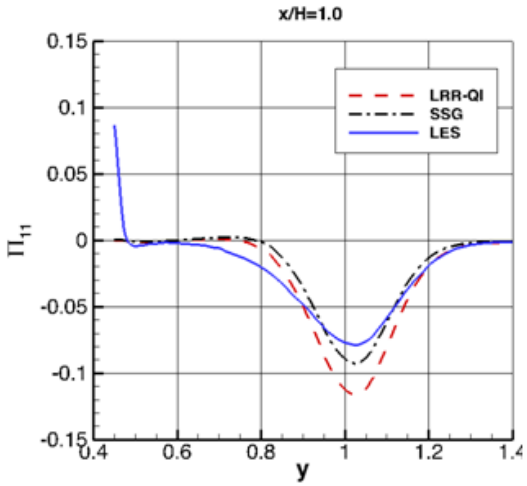


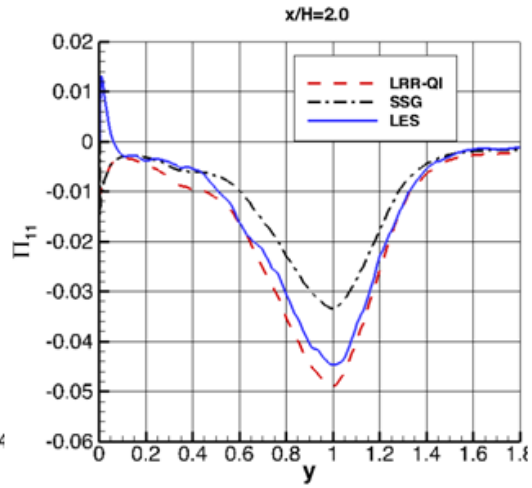


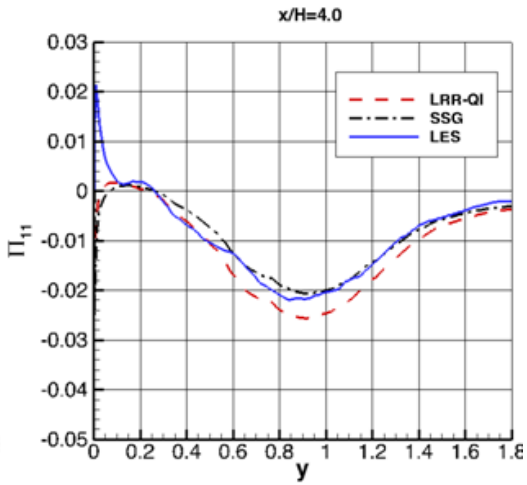

# *a-priori* studies of 2-D separation–Diffusion anisotropy

- Near-wall assumption of isotropy of dissipation introduces errors. Assuming the limit $d_{ij} = a_{ij}$, corrects the EARSM to $N = c_1 + \mathcal{P}/\varepsilon$.

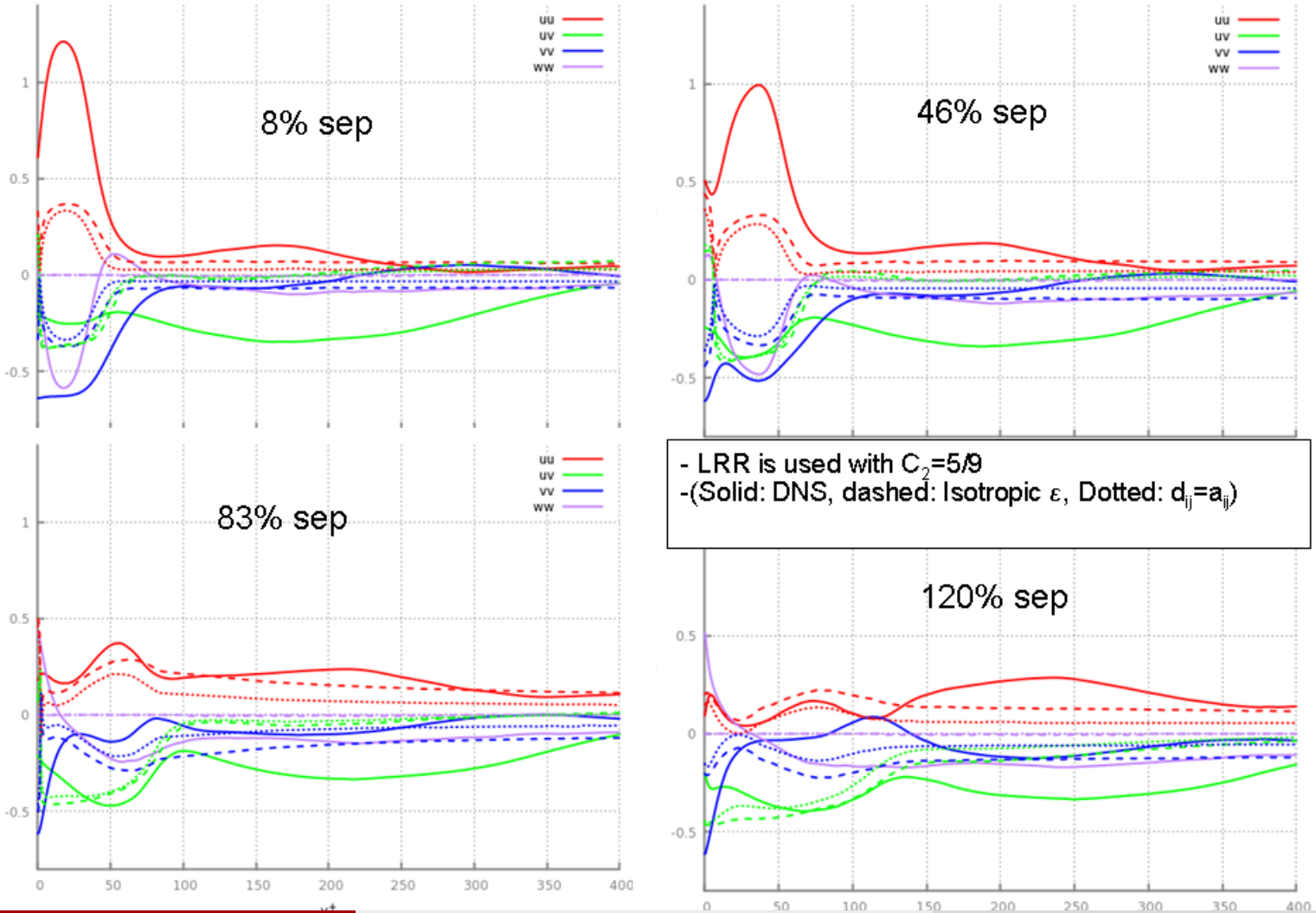

# Further conclusions

- EARSM predicts 3-D mean flow separation accurately in diffusers.
  - To predict near-wall quantities(pressure, etc) accurately wall modeling is required.
  - The Reynolds stress are under predicted.
- The errors in $\Pi_{ij}$ models are highest at start of separation. Wall models will not resolve discrepancies observed in high $\mathcal{P}/\varepsilon$ regions away from wall.
- Future work:
  - Elliptic blending to account for wall-blocking effects
  - Algebraic models for diffusion anisotropy.

Jochen Fröhlich, Christopher P. Mellen, Wolfgang Rodi, Lionel Temmerman, and Michael A. Leschziner. Highly resolved large-eddy simulation of separated flow in a channel with streamwise periodic constraint. *Journal of Fluid Mechanics*, 526: 19–66, 2005.

S. Lardeau, Y. Bentaleb, and M.A. Leschziner. Large Eddy Simulation of turbulent boundary-layer separation from a rounded step. to be published, 2011.

M. Marquillie, J.-P. Laval, and R. Dolganov. Direct numerical simulation of a separated channel flow with a smooth profile. *Journal of Turbulence*, Vol. 9, No. 1: 1–23, 2008.

Donghyun You, Meng Wang, and Parviz Moin. Large-Eddy Simulation of Flow over a Wall-Mounted Hump with Separation Control. *AIAA Journal*, 44, No. 11: 2571–2577, 2006.